HHS Public Access

Author manuscript

Environ Res. Author manuscript; available in PMC 2022 November 01.

Published in final edited form as:

Environ Res. 2021 November ; 202: 111557. doi:10.1016/j.envres.2021.111557.

Exposure to e-cigarette aerosol over two months induces accumulation of neurotoxic metals and alteration of essential metals in mouse brain

Diane B. Re[#1,2,3,‡], **Markus Hilpert**[#1,2], **Brianna Saglimbeni**[1,2,3], **Madeleine Strait**[1,2,3], **Vesna Ilievski**[1,2], **Maxine Coady**[1,4], **Maria Talayero**[1,2], **Kai Wilmsen**[1,4], **Helene Chesnais**[1], **Olgica Balac**[1,2], **Ronald A. Glabonjat**[1,2], **Vesna Slavkovich**[1,2], **Beizhan Yan**[2,5], **Joseph Graziano**[1,2], **Ana Navas-Acien**[1,2], **Norman J. Kleiman**[1,2,‡]

[1]Department of Environmental Health Sciences, Columbia University, New York, NY 10032, USA

[2]NIEHS Center for Environmental Health in Northern Manhattan, Columbia University, New York, NY 10032, USA

[3]Center for Motor Neuron Biology and Disease, Columbia University, New York, NY 10032, USA

[4]Master in Public Health Program, Environmental Health Sciences, Mailman School of Public Health, Columbia University, New York, NY, 10032, USA

[5]Lamont-Doherty Earth Observatory, Geochemistry Department, 203 Comer, 61 Route 9W - PO Box 1000, Palisades NY 10964-8000, USA

[#] These authors contributed equally to this work.

Abstract

Despite a recent increase in e-cigarette use, the adverse human health effects of exposure to e-cigarette aerosol, especially on the central nervous system (CNS), remain unclear. Multiple neurotoxic metals have been identified in e-cigarette aerosol. However, it is unknown whether those metals accumulate in the CNS at biologically meaningful levels. To answer this question, two groups of mice were whole-body exposed twice a day, 5 days a week, for two months, to either a dose of e-cigarette aerosol equivalent to human secondhand exposure, or a 5-fold higher dose. After the last exposure, the olfactory bulb, anterior and posterior frontal cortex, striatum, ventral midbrain, cerebellum, brainstem, remaining brain tissue and spinal cord were

[‡]**Corresponding authors:** Diane B. Re, 630 W 168th St, P&S Bldg. Suite 16-421B, New York, NY 10032, USA. dr2240@cumc.columbia.edu (**Editorial office contact**), Markus Hilpert, 722 W 168th St, ARB Suite 1107C, New York, NY 10032, USA. mh3632@cumc.columbia.edu, Norman J. Kleiman, 722 W 168th St, ARB Suite 1113, New York, NY 10032, USA. njk3@cumc.columbia.edu.

Declaration of Interests

The authors declare that they have no known competing financial interests or personal relationships that could have appeared to influence the work reported in this paper.

Experimental Animals

This study followed the National Institutes of Health "Guide for the Care and Use of Laboratory Animals (8th ed, 2011), and this work was reviewed and approved by the Columbia University Institutional Animal Care and Use Committee (IACUC #AAAU2471-NJK).

collected for metal quantification by inductively coupled plasma mass spectrometry and compared to tissues from unexposed control mice. The two-month exposure caused significant accumulation of several neurotoxic metals in various brain areas - for some metals even at the low exposure dose. The most striking increases were measured in the striatum. For several metals, including Cr, Cu, Fe, Mn, and Pb, similar accumulations are known to be neurotoxic in mice. Decreases in some essential metals were observed across the CNS. Our findings suggest that chronic exposure to e-cigarette aerosol could lead to CNS neurotoxic metal deposition and endogenous metal dyshomeostasis, including potential neurotoxicity. We conclude that e-cigarette-mediated metal neurotoxicity may pose long-term neurotoxic and neurodegenerative risks for e-cigarette users and bystanders.

Keywords

e-cigarette; aerosol exposure; metals; brain; neurotoxicity; metal accumulation

1. INTRODUCTION

Use of electronic cigarettes has increased over the past decade, particularly among youth (Pesko and Robarts, 2017), in part due to the perception that they are healthier and more “cool” than tobacco cigarettes (Brikmanis et al., 2017). However, much is unknown about the adverse human health effects of e-cigarette use (Kaisar et al., 2016). New data from our research group (Hess et al., 2017; Olmedo et al., 2018; Zhao et al., 2019) and others (Williams et al., 2017, 2013) raise concern that e-cigarette use may expose users and those in close proximity to toxic metals including nickel (Ni) and chromium (Cr), well-known inhalation carcinogens (Hess et al., 2017) and neurotoxicants (Nudler et al., 2009; Song et al., 2017). Other neurotoxic metals have been measured in e-cigarette aerosol at concerning levels. For example, we showed that levels of Ni, Cr, and lead (Pb) exceeded the U.S. Environmental Protection Agency national ambient air quality standards (NAAQS) or the Agency for Toxic Substances and Disease Registry minimum risk level (MRL) in >90% of our aerosol samples, and manganese (Mn) levels exceeded minimum risk levels in most aerosol samples (Zhao et al., 2019). Other metals of neurotoxic concern that have been found in e-cigarette aerosol by us and others in e-cigarette aerosols include selenium (Se), vanadium (V), copper (Cu), zinc (Zn), tungsten (W), uranium (U), tin (Sn), and recently, strontium (Sr) (Badea et al., 2018; Zhao et al., 2020).

Inhaled metals are known to be efficiently transferred into the brain via different routes including the nose-brain, the lung-brain and possibly the gut-brain pathways (Block et al., 2012; Lucchini et al., 2012; Sunderman, 2001). In the nasal cavity, metals can be deposited onto the neuroepithelium, to be transported along the olfactory nerves directly to the olfactory bulb, the most anterior part of the brain. The trigeminal nerve was also shown to directly transfer Mn via the nose-brain pathway in a rat model (Lewis et al., 2005). Some metals (e.g., Mn, Ni, Zn) were further shown to cross synapses in the olfactory bulb and migrate via secondary olfactory neurons to diverse areas of the brain including the amygdala, hippocampus, hypothalamus, thalamus, olfactory tubercle, pyriform and others (Sunderman, 2001). Other metals (e.g. Hg, Cd), however, were not observed to

cross synapses in the olfactory bulb. Their detection in deeper areas of the brain following inhalation exposure suggests other routes of transport such as from the distal lung alveoli into the blood or lymph before penetrating the blood brain barrier via various mechanisms and transport systems (Lucchini et al., 2012). Although the exact mechanisms remain elusive for many metals, distribution is thought to mainly occur via protein-bound intracellular transport along axons and across synapses between interconnected structures as well as via extracellular carriers and/or cellular uptake and efflux (Campos-Escamilla, 2021; Lucchini et al., 2012; Sunderman, 2001). E-cigarette use has been reported to damage the integrity of the blood brain barrier (Heldt et al., 2020), potentially leading to increased metal accumulation in the central nervous system (CNS), when compared to other sources of metal exposure. Many metals found in e-cigarette aerosol, including Cu, iron (Fe), Pb, Mn, mercury (Hg), Se and Zn, are known to cause various motor and cognitive deficits and are linked to adult-onset neurodegenerative diseases such as Alzheimer disease, Parkinson's disease, and amyotrophic lateral sclerosis (Cicero et al., 2017). Neurotoxic risks associated with inhalation exposure to e-cigarette aerosol are of particular concern for children and adolescents because of their developing brains (Giedd, 2008).

While a growing number of toxicological studies have examined potential e-cigarette adverse health effects such as cancer (Lee et al., 2018; Rowell et al., 2017), respiratory (Glynos et al., 2018; Larcombe et al., 2017) and cardiovascular (Farsalinos et al., 2013; Qasim et al., 2018) disease, few studies have examined neurotoxic effects, especially in controlled animal models. To date, most animal studies have focused on neurodevelopmental effects during early pregnancy or early-life exposure (Chen et al., 2018; Lauterstein et al., 2016; Nguyen et al., 2018; Zelikoff et al., 2018). In a small number of studies, adult mice exposed to e-cigarette aerosols showed adverse effects possibly related to metal overload and dyshomeostasis, such as oxidative stress in the frontal cortex (Kuntic et al., 2020), decreased dopamine levels in the striatum and frontal cortex (Alasmari et al., 2017), overall decreased brain glucose uptake and glucose transporters (Sifat et al., 2018), loss of blood brain barrier integrity and neurovascular inflammation (Kaisar et al., 2017), and brain lipid dyshomeostasis (Cardenia et al., 2018). However, the potential accumulation of e-cigarette aerosol-derived metals in the CNS and any potential associated dyshomeostasis in essential metals have not been investigated in rodent animal models. The present study fills this important knowledge gap. The findings are directly related to adult-onset neurodegenerative diseases like Alzheimer's and Parkinson's diseases, both of which are associated with profound metal dyshomeostasis (Chen et al., 2016; Cicero et al., 2017; Sussulini and Hauser-Davis, 2018) and whose development may be accelerated by chronic exposure to e-cigarette-derived neurotoxic metals.

In this paper, we report that e-cigarette aerosol exposure in an animal model results in neurotoxic metal accumulation as well as dysregulation of some endogenous metals in the CNS. Of the 15 metals/metalloids analyzed, six are essential elements necessary to vital physiological processes. Therefore, there is a biologically plausible pathway for CNS metal dyshomeostasis after chronic e-cigarette aerosol exposure that might increase neurotoxic and neurodegenerative risks. The findings of our study suggest an urgent need for additional investigations into the potential neurotoxic health effects of exposure to e-cigarette aerosol and will likely inform public health authorities, policy makers, and consumers about

additional neurotoxic health risks associated with e-cigarette use (Ferrea and Winterer, 2009; Ruszkiewicz et al., 2020).

2. METHODS

2.1. Animals

This study followed the National Institutes of Health "Guide for the Care and Use of Laboratory Animals" (8th ed., 2011), and the work was reviewed and approved by the Columbia University Institutional Animal Care and Use Committee (IACUC). Three randomized groups of five each, two-month old CD-1® IGS mice (Charles River Laboratories, MA, strain 022) were housed in micro-isolator cages in a temperature-controlled room (22–24°C) on a 12-hr light/dark cycle with ad libitum access to standard chow (PicoLab Rodent diet 20, LabDiet cat no 5053) and reverse osmosis filtered water. We elected to work on the outbred CD-1 mouse strain because it is genetically diverse and thus has a higher likelihood of results being translatable to humans when compared to inbred strains, as suggested by a previous study which examined systemic toxicity of chronic e-cigarette exposure (Crotty Alexander et al., 2018). Mice were acclimated for two weeks before e-cigarette aerosol exposure.

2.2. Mouse exposure and exposure system

Two groups of five each "low dose" and "high dose" mice were whole-body exposed twice a day, five days/week for two months to e-cigarette aerosol in a custom-built exposure chamber system we developed and described in previous work (Hilpert et al., 2019). Another group of five "controls" mice was exposed to HEPA filtered air. Our exposure system allows automatically puffing an e-cigarette at a programmable arbitrary puff topography, controlling the air exchange rate Q_{ex} in the chamber, and measuring aerosol concentrations c_m to which mice are exposed. In each exposure session, the low- and high-dose groups of 5 mice each were put into the exposure chamber at the same time. The low-dose cohort was removed from the chamber earlier than the high dose group to achieve the two doses described below. After 60 days, mice were euthanized for CNS tissue collection as described below.

We generated aerosol from a popular open-system e-cigarette (iStick Pico 25, Eleaf, Shenzhen, China). The e-cigarette was operated with a manufacturer-supplied "atomizer" head (part number HW2, with two heating coils), operated at an electrical power P = 40 W, within the manufacturer-recommended power range of 30 to 70 W. The puff time was T_{puff} = 2 s, and the puff period was 60 s. For the e-liquid, we used "Vixen's Kiss" e-liquid (Pale Whale, Baldwin Park, CA) with a labeled 0% nicotine content. Eleaf reports the HW2 coil is composed of a proprietary Kanthal™ alloy with Japanese organic cotton wicking surrounded by an aluminum (Al)-Zn alloy casing. Kanthal™ typically consists of Fe with substantial amounts of Al (5.8%) and Cr (20.5–23.5%), some Mn (0.4%), as well as carbon (C) and silicon (Si) (https://www.kanthal.com/en/products/).

We measured administered aerosol doses using real-time gravimetric analysis (Noël et al., 2018), because aerosol concentrations were too high to be measured with a previously used

real-time aerosol monitor (Hilpert et al., 2019). Air exchange was established by a stand-alone vacuum pump (JH12-65, 5L/min, DC 12V, −65kpa) powered by a variable voltage power supply (KORAD, KD3005D digital control, power 0–30 V, 0–5 A, Shenzhen Korad Technology, Shenzhen, China). Using a flow meter (TSI, 4100 Series, TSI, Shoreview, MN), the flow rate of the vacuum pump was set to Q_{ex} = 0.5 L/min. Flow rate was measured and logged periodically during each exposure session and, if needed, slightly adjusted to ascertain that gradual filter clogging did not substantially lower Q_{ex}.

To perform real-time gravimetric analysis, a filter holder containing a hydrophilic, mixed cellulose ester filter membrane (HAWP, 0.45 μm pore size, 37 mm diameter, Millipore-EMD, Danvers, MA) was inserted into the tubing line through which the vacuum pump withdrew aerosol-laden air from the chamber for air exchange. In previous research, we established that a membrane of this pore size retained the vast majority of aerosol (a membrane with half that pore size did not retain measurably more aerosol) (Hilpert et al., 2019). At pre-determined timepoints, we swapped the pre-weighed filter holder to measure the collected aerosol mass by weighing the filter holder containing the membrane on a micro-balance (XS105 DualRange, Mettler Toledo, Columbus, OH). From the time series of collected aerosol mass and the only slightly varying flow rate, we calculated the exposure time needed to achieve each dose, at which time mice were removed from the chamber.

To specifically characterize the metal concentrations in the aerosol administered to the animals, we collected e-cigarette aerosol in triplicate using a direct aerosol collection method (Hilpert et al., 2021; Olmedo et al., 2016) operating the e-cigarette device under identical conditions as those used for mouse exposure experiments.

2.3. Applied dose

Mice were exposed to two different aerosol doses D (mg/m^{-3}·min) which we defined as the time-integrated aerosol concentration in the exposure chamber: $D = \int_0^t c_m(t')dt'$ where c_m (mg/m^3) is the aerosol concentration to which the mice were exposed in the exposure chamber, and t (min) is the duration of exposure.

Doses were chosen based on measured environmental (second-hand) e-cigarette aerosol concentrations. There is significant variability in reported environmental aerosol concentrations with levels ranging from 30 to 800 μg/m^3 (Czogala et al., 2014; Jamal et al., 2017; Saffari et al., 2014; Soule et al., 2017) due to many influencing factors including device type, number of e-cigarette users and room size and ventilation. The two doses we administered to the mice were based on the median environmental $PM_{2.5}$ level measured at an e-cigarette event, c_{env} = 0.819 mg/m^3 (Soule et al., 2017). To account for the different physiologies of humans and mice, we sought to match the daily inhaled aerosol dose normalized by body weight, m_{daily}/m_{body}. For an adult human, we assumed 24 hours of daily exposure, a minute ventilation MV_h = 6 L/min, and a body weight m_h = 70 kg. Thus, $\frac{m_{daily}}{m_{body}} = \mathrm{MV}_h \times c_{env} \times 1,440 \quad \mathrm{min}/m_h = 0.101\,\mathrm{mg/kg}$. We chose to expose mice two times per day and five days per week. Matching m_{daily}/m_{body} between humans and mice now yields the following constraint for the dose D that was administered to the mice in each session:

$$D = \frac{1}{2}\frac{7}{5}\frac{m_{daily}}{m_{body}}\frac{m_m}{\mathrm{MV}_m} \quad (1)$$

where the factor of 1/2 accounts for the two exposure sessions per day, the factor of 7/5 accounts for five days of exposure per week, m_m is the body weight of the mouse, and MV_m is the minute ventilation rate of the mouse.

Assuming a minute ventilation per mouse body weight of $\mathrm{MV}_m/m_m = 1.1$ mL·min^{-1}·g^{-1} (Tankersley et al., 1994), this dose is $D = 64$ mg/m^{-3}·min. However, we used a "low" dose that was about 150 times higher, i.e., $D_{low} = 10{,}000$ mg/m^{-3}·min to account for an animal-to-human uncertainty factor of 100 (Dankovic et al., 2015; Dorne and Renwick, 2005) used, e.g., for Mn (ATSDR, 2012). To improve statistical power, a second cohort of mice was exposed to a dose five times higher, i.e., $D_{high} = 50{,}000$ mg/m^{-3}·min.

For the high dose, exposure sessions lasted typically about 45 min, which corresponds to an average aerosol concentration of ~1,000 mg/m^3, a value much higher than the measured environmental aerosol concentration of 0.819 mg/m^3 on which we based our administered doses. As described above, the three orders magnitude in difference can be attributed to the animal-to-human uncertainty factor and the shorter exposure time for the mice.

2.4. Blood, brain and spinal cord collection and dissection

After two months of exposure, mice in all three groups (low and high dose, as well as unexposed controls) were deeply anesthetized with ketamine/xylazine, and blood was collected by cardiac puncture followed by immediate euthanasia by decapitation. Based on precise mouse cortical anatomy (Bizon et al., 2012; Ebbesen et al., 2018) and using published methodology (Jackson-Lewis and Przedborski, 2007), the following brain areas were identified and dissected: olfactory bulb; anterior frontal cortex (including prefrontal cortex and facial motor areas); motor-somatosensory cortex (including trunk and limb motor areas and frontolateral somatosensory areas); striatum; ventral midbrain (containing mainly substantia nigra and ventral tegmental area); brainstem and cerebellum. The remainder of the brain was pooled and labeled as remaining brain tissues. To collect the spinal cord the spinal column was isolated after decapitation and removed from the body. The spinal cord was then flushed using published methods (Richner et al., 2017). All tissue samples were weighed before being placed in barcode-labeled 15 mL metal-free centrifuge tubes (Labcon, Petaluma, CA). Tubes were frozen and stored at −80°C until assayed for metal content.

2.5. Metal analyses

Tissue samples were analyzed for 15 different metals/metalloids in the Columbia University Trace Metals Laboratory using a Perkin-Elmer NexION 350S with Elemental Scientific Autosampler 4DX. Inductively coupled plasma mass spectrometry (ICP-MS) dynamic reaction cell methodology was developed from published methods (Cesbron et al., 2013; Nixon and Moyer, 1996; Stroh, 1993) and modified as per Perkin-Elmer's suggestions. Although considered essential, 6 of the metals analyzed (bolded) pose neurotoxic potential at high concentrations (Mehri, 2020). The other 9 metals/metalloids are considered neurotoxic at lower levels (Chen et al., 2016): arsenic (As), Cr, **Cu**, **Fe**, **Mn**, **Ni**, Pb, Sb,

Se, Sn, Sr, Thallium (Tl), V, W and **Zn**. E-cigarette aerosol concentrations for some of these metals were previously reported by us using the same e-cigarette but a different coil (open device 1; iStick Pico 25 in (Zhao et al., 2019)). In the present study, we added Tl, Se and V due to their neurotoxic potential (Chen et al., 2016; Ngwa et al., 2017; Vinceti et al., 2014) and presence in tobacco cigarette smoke or e-cigarette aerosol (Ghaderi et al., 2018; Williams et al., 2017). We also added Sr as it was recently detected in e-cigarette aerosol (Badea et al., 2018).

Tissue samples were digested in 1 mL of HNO_3 (Fisher *OPTIMA Grade*) before addition of 100 μL of internal standards and dilution with distilled water to 10 mL. After centrifugation for 10 min at 3,500 rpm (2,450 × g), an aliquot of the supernatant was analyzed. A standard solution chosen to cover the expected range of metal concentrations in the samples was used for instrument calibration. Matrix-induced interference was corrected by selecting appropriate internal standards to match the mass and ionization potential of the chosen analytes. We added rhodium (Rh), lutetium (Lu), gallium (Ga), and iridium (Ir) to all calibrators and samples at the same concentration, about 10 ng per tube. Polyatomic interference was suppressed with the instrument's dynamic reaction cell technology, which utilizes oxygen or ammonia as a second gas.

Blood measurement of toxic metals was done following the method developed in our laboratory based on published methods (Chen et al., 1999) modified and adjusted in collaboration with Perkin Elmer application specialists. Simultaneous determination of all metal concentrations was done by diluting blood samples, calibration standards, and quality control (QC) samples with diluent (2% HNO3 + 1% Ethanol + 0.02% Triton X-100), adding internal standards (Ga, Rh, Ir), and centrifuging the blood samples and QCs before runs. Samples were run in two modes, standard and dynamic reaction cell (DRC). Standard mode was used for Sb, Cu, Pb, Ni, Sn, W, and Zn, while DRC mode for Cr, Fe, Mn, and As. The second gas used in DRC mode was oxygen for As, and ammonia for Cr, Fe, and Mn (Chowdhury et al., 1997; Pruszkowski et al., 1998).

After instrument calibration and throughout the day, QC samples were run, and the instrument was recalibrated based on those runs. QC samples are blood samples with known analyte concentrations obtained from the Laboratory for ICP-MS Comparison Program run by the Institut de Santé Publique du Quebec. Method detection limits (MDL), Method Quantitation Limits (MQL) as well as the numbers of MDL and MQL deceedances are listed in Table S1 for tissues and human blood.

2.6. Statistical analyses

For descriptive statistics, box plots were generated for metal concentrations measured in the five mice for each of the three exposure groups (control, low dose, high dose) stratified by metal and tissue type. In box plots, squares and circles indicate values below and above MDL, respectively. Significance of the differences between the three unmatched exposure groups was assessed based on the Kruskal-Wallis test followed by a Dunn test and a p=0.05 significance level. In all analyses, samples below the MDL were not imputed by replacing them by a fixed threshold (e.g., $MDL/\sqrt{2}$) (Whitcomb and Schisterman, 2008). For each

metal, extreme outliers were identified for concentrations of all 15 mice combined according to the 3 × inter quartile range (IQR) rule and removed (Beyer, 1981).

Statistical analyses were performed with R version 4.03.

3. RESULTS

In the following subsections, we report metal concentrations measured in e-cigarette aerosol and mouse tissues after 2-month exposure to e-cigarette aerosol. For the aerosol, we present data for all the 15 metals/metalloids we measured. For four out of the nine CNS areas examined and for blood, we depict concentrations of only 10 elements (As, Cr, Cu, Fe, Mn, Ni, Pb, Se, Sr, and Zn) in subsequent figures and tables. We do not report levels of Sb, Sn, Tl, V and W, because a high proportion of samples (≥ 29%) were below their respective MQLs (Table S1). We also do not report Tl because it was not detected above its MDL in e-cigarette aerosol (Figure 1) or e-liquid (data not shown).

For reference, the data for the remaining five CNS areas are shown in Figures S1–S5, and the raw data for Sb, Sn, Tl, V and W in blood are provided in Table S2. Finally, Figures S6–13 present across all nine CNS areas examined for each of the 15 metal/metalloids individually measured concentrations and stratified by exposure group.

3.1. E-cigarette aerosol metal content

Figure 1 shows metal levels measured in aerosol generated by the e-cigarette used in the animal exposure experiments and operated under identical conditions of power and puff/interpuff time. Metals that are part of the heating coil alloy, namely Cr, Fe and Mn, were found at significant levels above their respective MDLs. Fe levels were about two orders of magnitude higher than Mn levels, mirroring the ratio in typical Kanthal™ coil alloys. Fe levels were also about two orders of magnitudes higher than Cr levels but did not mirror the ratio of 3 in the coil. Zn levels were second-highest, even though Zn is not a known component of Kanthal™. Overall, aerosol metal levels were either similar (As, Fe, W) or lower (Cr, Cu, Mn, Ni, Pb, Sn, Zn) when compared to a previous study of the same device operated with a different coil and different e-liquids (Zhao et al., 2019).

3.2. Blood metal levels

After the 2-month exposure, levels of some metals were significantly increased in the mouse blood in the e-cigarette aerosol exposed groups compared to controls (Table 1). Levels of metals known to be present in the Kanthal™ heating coil alloy (Cr, Fe and Mn) were significantly increased in blood from e-cigarette exposed animals when compared to the control group. For Cr, blood levels were 41% higher in the low-dose and 31% in the high-dose group (Table 1; p=0.01 for both). For Fe, blood levels were significantly higher only in the high-dose group by 7% (p=0.03). Although Mn and Se blood levels increased in both exposed groups, statistically significant increases were only found in the low-dose group: 28% for Mn (p=0.01) and 10% for Se (p=0.05). The only metal that was found to be significantly decreased in blood was Pb in the high dose group (p=0.02).

3.3. Olfactory bulb metal levels

Inhaled metals can find their way to the brain either by passage through the lung and blood brain barrier or via the nasal passages into the olfactory bulb (Gardner et al., 2017). At the end of the 2-month exposure, we found that Cu (+23%) levels in the olfactory bulb were significantly higher in the high-dose than the control group (Figure 2; p=0.004).

Zn (−26%) and Se (−27%) levels were significantly lower in the low-dose than in the control group (p=0.01 and p=0.04, respectively; Figure 2).

3.4. Anterior frontal cortex metal levels

In rodents, the anterior frontal cortex includes the prefrontal cortex, which, while less developed than in the human brain, is implicated in complex cognitive tasks and executive function (Bizon et al., 2012). Moreover, this region is involved in the control of the muscles of the jaw, lips, tongue, rhinarium and vibrissa (Ebbesen et al., 2018). As illustrated in Figure 3, we found a significant accumulation of Cu (+14%; p=0.03) and Zn (+14%; p=0.01) in the anterior frontal cortex of the high-dose group, while Sr was increased in both exposure groups (+39%; p=0.01; and +38%; p=0.02, respectively). In contrast, Se (−14%) and Mn (−9%) were both significantly decreased in the low-dose group (p=0.03 for both) as compared to the controls. In agreement with the data found in the olfactory bulb (Figure 2), this indicates that while accumulation of metals in the low-dose group was not significant (except for Sr), clear signs of metal dyshomeostasis are observed for some essential metals with some degree of tissue-specificity, as Zn and Se were also depleted in the olfactory bulb while Mn was depleted in the anterior frontal cortex (Figure 3). In contrast, Pb (−24%; p=0.04) levels were significantly decreased in the high-dose group as compared to controls.

3.5. Striatum metal levels

The striatum exhibited the most widespread and striking changes in metal levels following e-cigarette aerosol exposure. This brain area, which is critical to movement control, action selection and reward learning (Prager and Plotkin, 2019), demonstrated significant increases in both the low- and high-dose groups for several metals as well as increases in the high-dose group alone for others (Figure 4). Dose-dependent increases occurred for Cu (+16 and 42%; p=0.02 and 0.001, respectively for low- and high-dose), and Sr (+83 and 99%; p=0.01 and 0.003, respectively. As (+43 and 36%, in the low- and high-dose group, respectively; p=0.01 for both) was increased in both dose groups. Metals which exhibited increased levels in the high-dose group alone include Fe (+26%; p=0.01), Mn (+18%; p=0.05), Pb (+185%; p=0.01), and Se (+31%; p=0.02). With the exception of Se, for which levels of the low-dose group were lower than those of the control (though not significantly), all median metal levels were higher in the low- and high-dose groups than in the control group indicating metal accumulation in the striatum.

3.6. Ventral midbrain metal levels

The ventral midbrain contains almost 75% of all dopaminergic neurons in the adult CNS in two main dopaminergic structures, the substantia nigra and the ventral tegmental area, which are, respectively, crucial for movement control and reward cognition (Hegarty et al., 2013). The substantia nigra is known to accumulate metals with age and to have increased metal

levels in neurodegenerative disease conditions such as Parkinson's disease (Bjørklund et al., 2020; Jiang et al., 2019). A significant accumulation in the low-dose group was found for Ni (+39%; p=0.04) and Sr (+87%; p=0.01) (Figure 5).

We also observed a depletion of two metals essential for physiological antioxidant enzyme function: Se (−14% in both dose groups; p=0.04 and p=0.03, in the low- and high-dose group, respectively) and Zn (−7% in the high-dose group; p=0.04).

3.7. Metal levels in other mouse CNS areas

Metals with neurotoxic potential also significantly accumulated in other CNS areas. In the motor-somatosensory cortex, we observed increases in Cr (+61% in the low-dose group, +112% in the high-dose group; but increases were significant only in the low-dose group with p=0.04 and p=0.07, respectively) and Pb (+259% in the low-dose group; p=0.01) levels (Figure S1). In the Cb, we observed increases in Zn (+8%; p=0.05) levels for the high-dose group (Figure S2). In the brain stem, we observed increases in Fe (+20%; p=0.003) and Pb (+126%; p=0.04) levels for the high-dose group (Figure S3). In the spinal cord, we observed increases in Ni (+28%; p=0.05) levels in the low-dose group (Figure S4).

We also measured metal levels in the pooled remaining brain (Figure S5), which notably includes the rest of the parietal and occipital cortex, the hippocampus, the thalamus, hypothalamus and basal forebrain. We found significant increases in both dose groups for Fe (+17% and +10%; p=0.004 and 0.04, for low- and high-dose groups, respectively), Mn (+9% and +14%; p=0.04 and 0.02 for low- and high-dose groups, respectively) and Zn (+11% and +13%; p=0.01 and 0.003). The pooled remaining brain also revealed significant increases for the high-dose group for As (+15%; p=0.03), Cu (+13%; p=0.03) and Se (+17%; p=0.001). This suggests that these brain areas exhibit significant metal level increases after only 2 months of exposure that deserve to be studied separately in future investigations.

Significant decreases in various metals (essential or not) were observed in the spinal cord: As (−19% and −15%; p=0.01 and 0.04 in the low- and high-dose group, respectively), Cu (−14% and −11%; p=0.02 and 0.04), and Se (−16% and −12%; p=0.01 and 0.02) (Figures S4).

3.8. Distribution and bioaccumulation of metals

The concentrations of the different metals measured in this study vary substantially (up to 6 orders of magnitude) within given tissue samples and to a lesser but still remarkable extent (up to 1 order of magnitude) for the same metal across CNS areas (see range of detection for each metal across treatment groups given in Table 2). The high variability in concentration between different metals can primarily be attributed to whether the metals are essential elements, which have important biological roles and are typically present at high endogenous levels, like Zn or Cu, or xenobiotic metals, which do not have a biological role and are typically present at trace levels, like As or Pb. For the same metal the variability between CNS areas and treatment groups, can be extensive e.g., 8–24 μg/g (range of values reported for Zn in Table 2; see also Figure S13). If we take the example of Zn in controls, levels are much lower in the ventral midbrain, brain stem and spinal cord (~10 μg/g) as compared with the upper and more anterior areas of the brain like the olfactory bulb,

striatum, cortex (~16 μg/g). Others have previously reported an important variability of Zn levels in mouse brains (Tonge, 2017). The origin of Zn level variability between CNS areas remains elusive. However, we can hypothesize that it is driven by variable levels in Zn binding proteins between these diverse areas, knowing that most Zn is protein-bound in the brain (Portbury and Adlard, 2017).

To characterize better how the various metals partition and accumulate differently in the same tissue and how the same metal partitions and accumulates differently across the CNS, we calculated for each metal-tissue combination the following "partitioning ratio:"

$$R = \frac{c_{high} - c_{control}}{c_{aerosol}} \quad (2)$$

where c_{high} and $c_{control}$ are the mean metal concentrations of the high-dose and control group, respectively, and $c_{aerosol}$ is the metal aerosol concentration.

For xenobiotic metals with no biological roles, we would typically expect R to be smaller than one, because only a fraction of the inhaled aerosol is absorbed by the body and the complex pharmacokinetic processes within the mouse body can be expected to lower the levels of metals that reach the brain even further. However, if a metal is not eliminated efficiently upon absorption, it will, upon repeated exposure, bioaccumulate, and the ratio may become higher than one. For most endogenous essential metals that are not particularly concentrated in e-cigarette aerosol, we would expect the ratio to be greater than 1 and to potentially increase upon repeated exposure. Metal-tissue combinations for which the ratio according to Equation (1) is high and positive will be indicative of enhanced bioaccumulation of the metal in the tissue. A negative ratio means that the tissues exposed to e-cigarette aerosol have lower metal levels than the controls indicating that higher exposure levels trigger extrusion of specific metals probably due to compensatory mechanisms linked to increase in other metal levels.

Figure 6 shows the ratio according to Equation (1) for all metal-tissue combinations for which the ratio is significantly positive (confidence intervals do not include 0). As illustrated, Cu shows the highest potential for bioaccumulation (~1,000 fold) in the striatum and the anterior frontal cortex, followed by Fe (~100 fold) in the striatum and the brain stem. In the same range, Se and Zn bioaccumulate (~50–100 fold) in the anterior frontal cortex, and Se in the striatum (~100 fold). Sr bioaccumulates (~5–10 fold) in the anterior frontal cortex and striatum, suggesting that these two brain structures important in executive functions and connected by frontostriatal circuits (Alexander et al., 1986) are metal sinks following e-cigarette aerosol exposure. Finally, As levels in the striatum and brain stem, respectively, were similar to those in the aerosol (R=1).

We also performed principal component analysis (PCA) with results shown in Section A in the Supplementary Material. Overall, PCA of the distributions of metals in the 15 mice confirmed the dose responses observed in the box plots for certain metals individually.

4. DISCUSSION

4.1. Metal accumulation in CNS

We provide the first experimental evidence that a relatively short sub-chronic exposure (2 months, twice a day, 5 days a week) to e-cigarette aerosol causes significant accumulation of various neurotoxic metals in several areas of the mouse CNS, most notably the striatum and anterior frontal cortex. The metals showing accumulation in at least one part of the brain included As, Cr, Cu, Fe, Mn, Ni, Pb, Se, Sr and Zn (Table 2).

It remains unclear whether the metal- and region-specific accumulations that we observed in the brain of mice exposed to e-cigarette aerosol are only due to increased entry or also to impaired elimination. Most metals (like Mn and Fe) are known to accumulate in the brain due to their slow excretion in this organ, a key determinant in their preferential neurotoxicity (Fernsebner et al., 2014). Metals are slowly eliminated from the brain because, in contrast to their entry, facilitated by specific transporters, metal efflux is not mediated by carriers but rather dependent on slow diffusion process controlled by bulk cerebrospinal fluid flow (Yokel et al., 2003; Zheng et al., 2003). One exception is Pb which was proposed to be pumped out of the brain back to the circulation via a Ca^{2+} -ATPase (Deane and Bradbury, 1990).

Overall, the metals we found to be significantly increased in blood from exposed mice (Table 1) (Cr, Fe, Mn, and Se) were different from those increased) in olfactory bulb (Figure 2) (Cu only). Remarkably, metal concentrations in blood and olfactory bulb were not predictive of these metal levels in other CNS structures. In our metal bioaccumulation analysis (Figure 6), we observed that some metals accumulated to comparable extent in brain areas interconnected by axonal projections (e.g., Cu in olfactory bulb and striatum (Hintiryan et al., 2012) and Se and Sr in striatum and anterior frontal cortex (Alexander et al., 1986). However, this was not the case for most metals, whose levels were dissimilar and not predicted either by anatomical or functional connections. We conclude, therefore, that upon exposure to e-cigarette aerosol metal mixtures, CNS area-specific metal content is likely determined by a complex interplay between several routes of metal entry, local mechanisms of metal retention and elimination, as well as potential positive and negative interaction between metals sharing common or interrelated metabolic pathways, for example those reported for Mn and Fe, Mn and Pb, As and Pb, or As, Mn and Pb (Chen et al., 2016; Fitsanakis et al., 2010). These interactions potentiate synergistic neurotoxic effects in rodent models (Chen et al., 2016) that may be particularly relevant to brains exposed to e-cigarette aerosol especially those striatal area where these 4 metals (As, Fe, Mn and Pb) were all found to be significantly increased (Figure 4). In future studies, it is important to determine the potential deleterious effect(s) of chronic e-cigarette on the blood brain barrier (Heldt et al., 2020) and nasal epithelium integrity (Sunderman, 2001) and how this many influence the balance between metal CNS entry and elimination.

Toxic metals accumulation in tissues can also be modified by essential element abundance in the diet. Such interactions were found to occur between Ni and Cu, As and Cu, and As and Mn in rats exposed to toxic and essential dietary metal excess (Elsenhans et al., 1987). As e-cigarette aerosol contains elevated levels of both toxic and essential metals, competition

between them may have occurred in our experimental paradigm and this may account for some of the variability in metal accumulation across the various CNS areas investigated.

Many of the metals we found to accumulate in e-cigarette aerosol-exposed mouse CNS are well known for their neurotoxicity. For instance, chromium overexposure causes dizziness, headaches and weakness in humans (Lieberman, 1941) and decreased locomotor activity in rodents (Salama et al., 2016), although the long-term neurotoxic effects of chronic moderate exposures in humans and animal models are not well characterized. Cr levels were significantly increased in the motor-somatosensory cortex and almost significantly increased in the ventral midbrain and brain stem (Figure S6b). In the present study, we measured total Cr, but this metal mainly occurs in two stable forms: Cr(III) and the more toxic Cr(VI) (Outridge and Scheuhammer, 1993). In future work, it will be important to perform Cr speciation analysis on e-cigarette aerosol to untangle the effects of Cr valencies. Such work is challenging, however, as after crossing biological membranes and entering cells, Cr(VI) is rapidly reduced to Cr(III) with corresponding generation of reactive oxygen species (Petrilli et al., 1986). Inhaled Cr can be transported directly to the brain via the olfactory and trigeminal nerve pathway, and studies in mice and rats have demonstrated that 60% increases in brain Cr at levels similar to those we measured (0.1 μg/g) were associated with oxidative stress, gliosis and neurodegeneration (Salama et al., 2016; Travacio et al., 2001).

Copper is an essential element with neurotoxic oxidative potential at both high and low levels (Bulcke et al., 2017). Cu levels were increased in the olfactory bulb, anterior frontal cortex, striatum and remaining brain (Figure S7a). Among those, the 42% Cu increase in the striatum at high dose is particularly worrisome, because smaller increases (~+29%) had profound deleterious effects on mood-related and movement behaviors in a mouse model of Wilson's disease (Han et al., 2020), a genetic disorder leading to Cu deposition in multiple brain regions including the dorsal striatum, thalamus, brain stem, and frontal cortex (Brewer and Yuzbasiyan-Gurkan, 1992; Meenakshi-Sundaram et al., 2008). Although the maximal increase that we measured in Zn levels in the anterior frontal cortex (+14.5%) of mice exposed to e-cigarette aerosol is not predicted to be neurotoxic based on previously studies (Luo et al., 2009), Cu was also found to accumulate in the anterior frontal cortex. This co-occurrence of Zn and Cu in the anterior frontal cortex could be relevant since some calcium channels involved in epilepsy ($Ca_v2.3$) are tightly controlled by endogenous trace metal cations like Cu^{2+} and Zn^{2} (Alpdogan et al., 2020), and the progressive accumulation of these 2 essential metals in vulnerable regions of the brain could potentially explain the increased frequency of epileptic seizures reported among some e-cigarette users (Wharton et al., 2020).

Iron is highly redox active essential metal that, via the Fenton and Haber Weiss reaction, can generate damaging free radicals (Kanti Das et al., 2014). Thus, Fe levels are highly regulated physiologically (Kozlowski et al., 2014). In the high-dose group, Fe showed the greatest increase in the striatum (+27%) followed by the brain stem (+20%). Fe also increased in both dose groups in the remaining brain (+17 and +10%). Consistent with the highest increase in the striatum observed in this study (Table 2), others reported iron oxide nanoparticle accumulation in the striatum following experimental inhalation exposure (Imam

et al., 2015; Wu et al., 2013). This is plausible since some of the Fe in the e-cigarette aerosol might have been present as nanoparticles, a conclusion supported by a microscopic analysis of e-cigarette aerosol (Williams et al., 2013). The Fe increases we observed are of concern since two studies that exposed rodents orally to 2.5 mg/kg Fe-succinate demonstrated that a reported 16% increased Fe accumulation in the CNS resulted in long-lasting learning memory deficit in rats (Schröder et al., 2001) and a locomotion deficit in mice (Fredriksson and Archer, 2003).

Manganese is an essential element that at high levels can cause “manganism”, a disorder resembling Parkinson’s disease, and is suspected to be implicated in the etiology of several neurodegenerative diseases (Bowman et al., 2011). Similar to our findings for Cu and Fe, the highest increase of Mn occurred in the striatum (+18%) which is known to be particularly rich in divalent metal transporter 1 (DMT-1), explaining why divalent metals (e.g. Cu^{2+}, Fe^{2+}, Mn^{2+}, Pb^{2+}) tend to accumulate in this structure (Burdo et al., 1999). Consistent with our findings, Mn is known to reach primarily the striatum and the prefrontal cortex upon inhalation (Antonini et al., 2010; Elder et al., 2006; Ye and Kim, 2016). Of concern, similar accumulation of Mn in the CNS (+19%) resulted in significant locomotor and emotional deficits, as well as glial activation in mice chronically exposed to Mn via drinking water (Krishna et al., 2014). Several studies in wild-type, Alzheimer’s model and aging mice reported that increased DMT1 expression could also explain the accumulation of Fe in the mouse pre(anterior) frontal cortex; for review see (Ingrassia et al., 2019).

Lead is especially neurotoxic in the developing brain. Numerous human studies report adverse effects of childhood Pb exposure on IQ and cognition, and experimental studies in rodents and nonhuman primates demonstrated that developmental Pb exposure is linked to the development of Alzheimer disease later in life (Caito and Aschner, 2017). We found the highest increase in Pb levels in the striatum (+185%), followed by the brain stem (+126%). Comparable percentage increases of Pb in the CNS (+200%) were reported to cause glial inflammation in the brain of developmentally-exposed mice (Li et al., 2015).

Levels of other metals including Ni (+39%) and Sr (+99%) were significantly increased in the CNS of e-cigarette aerosol-exposed mice (Table 3). However, these data are more difficult to interpret due to the limited literature. For instance, intraperitoneally injected Ni(II) oxide nanoparticles triggered signs of neuronal injury at levels at which there were no significant increases in brain Ni levels (Minigalieva et al., 2015). Even though another study identified Ni nano-particles in e-cigarette aerosol (Williams et al., 2013), it is unclear whether e-cigarette aerosol-borne Ni was present in the Ni(II) oxidation state. Experimental studies in mice that investigated Ni neurotoxicity utilized high exposure levels, leading to massive increase of brain Ni (+102%) (He et al., 2013); we observed some more modest increases in the present study (maximum of +39%; Table 2). For Sr, while its role in synaptic release and neurotransmission has extensively been studied (Zhang et al., 2017) and subchronic Sr exposure was reported to cause paralysis of the hindlimbs in weanling male rats (Johnson et al., 1968), we found no measurement of Sr levels in mouse CNS wet weight tissue or any report of quantitative Sr changes associated with adverse effects that might help valiancy the potential neurotoxicity of the increased Sr levels observed (+99% in the striatum; Table 2). In mouse brain, dry weight tissue Sr was reported to average 0.37 μg/g

dry and rat brain about 0.30 μg/g dry (Takahashi et al., 2001). The only direct comparison we can make is that the levels of Sr we measured here in the CNS (0.09–0.6 μg/g wet) are overall below or equal to levels reported in rat brain (0.5 μg/g wet) (Skoryna, 1981) or human brain tissue (~0.263–0.281 μg/g wet) (Cilliers and Muller, 2020).

Other metals like As, Se and Zn significantly accumulated in mouse brain upon e-cigarette aerosol exposure (Table 2) but their respective increases were not predicted to have neurotoxic consequences based on previous experimental studies in mice (Luo et al., 2009; Panter et al., 1996; Yang et al., 2013).

4.2. Metal depletion in CNS

While overall e-cigarette aerosol-mediated metal depletions were less striking than metal accumulations in our study, depletion of essential metals and sometimes xenobiotic metals was observed in several areas.

Regarding essential metals, in the olfactory bulb, Se depletion (−27%) reached levels close to those previously reported to be of neurotoxic concern with respect to Huntington's disease (Huntington's disease; −30%) (Lu et al., 2014; Watanabe and Satoh, 1994). The olfactory bulb is one of the brain regions with the highest expression of selenoproteins (Zhang et al., 2008), which are known to counteract the toxicity of heavy metals by sequestering them and limiting metal-catalyzed oxidative stress. Se was also significantly depleted, but to a lower extent than in the olfactory bulb), in the anterior frontal cortex (low dose), ventral midbrain (both doses), brain stem (low dose), and spinal cord (both doses) (Figure S10a). Our data suggest that Se-dependent detoxification mechanisms could be impaired in the olfactory bulb and in key executive and motor control regions of the CNS of e-cigarette exposed subjects.

Likewise, we found significantly decreased Cu levels in the spinal cord of exposed mice (~−14%) at the two exposure doses, a value close to the −20% decrease in brain Cu levels reported in Menkes disease (an early fatal copper metabolism disorder) patients and mouse models (Bulcke et al., 2017). Zn depletion was also near significant in the spinal cord and significant in the ventral midbrain and olfactory bulb, where it was the highest ~−26% (see Table 2 and Figure S13b).

Finally, Mn showed a significant depletion in the anterior frontal cortex only at the low dose (−9%; Table 2) and this level of depletion is not predicted to have neurotoxic consequences based on previous data that showed adverse effects are reached at more profound levels of depletion (Frazzini et al., 2018). In contrast with Se, Cu and Zn, Mn depletion was only observed at low dose and in a single area. At higher dose Mn rather tends to or significantly accumulates in most CNS areas (Figure S8a). Therefore, in the context of long-term exposure to e-cigarette aerosol we can anticipate that accumulation rather than depletion of Mn may become a problem.

Regarding non-essential metals, Pb was found to be significantly decreased in the high dose exposure group in the anterior frontal cortex (Figure 3). In this brain area, all other metals rather tended to accumulate, this raising suspicion that selective depletion of Pb in the

anterior frontal cortex may be due to the activation of regionally expressed Ca^{2+} -ATPases that pump Pb selectively out of the brain back to the circulation (Deane and Bradbury, 1990). Longer chronic exposure studies may indicate whether this depletion is maintained over time.

Arsenic is the only other xenobiotic metal that was significantly decreased in the cerebellum and brainstem (low dose) and in the spinal cord (both doses) of e-cigarette aerosol-exposed mice compared to controls (Figure S6a). As depletion appeared to be always coupled to a decrease in Se, although it was significant in the brainstem (Figure S3) and spinal cord (Figure S4) but not in the cerebellum possibly due to an outlier (pink mice; Figure S2). Interestingly, Se and As chemical properties such as valence shells, electronic structures and atomic radii are very similar, and both are known to be substrates of the same transporters and exporters (Rosen and Liu, 2009). Therefore, we can hypothesize that As elimination/detoxification mechanisms could be responsible for a concurrent Se depletion.

4.3. Summary

Cr, Cu, Fe, Mn and Pb accumulated in the CNS at levels comparable to those previously associated with neurotoxic effects ranging from cognitive and/or motor deficits to pathological insults. These metal accumulations are of neurotoxic significance individually. The accumulation of Cu, Fe, Mn and Pb at neurotoxic levels in the striatum of mice exposed to e-cigarette aerosol is concerning for brain health of e-cigarette users and bystanders because (1) the doses we used in these animal experiments are based on environmental e-cigarette aerosol levels, and (2) both in the mouse and human brains the olfactory system is highly connected to the ventral and dorsal striatum (Zhou et al., 2019). In addition to being implicated in late-onset neurodegenerative diseases like Parkinson's disease, Huntington's disease, frontotemporal, and semantic dementia (Halabi et al., 2013; Nopoulos, 2016; Zhai et al., 2018), dysfunctions and damages to the striatum are involved in a myriad of neurological disorders including addiction, bipolar disorders, depression, obsessive compulsive disorders and autism spectrum disorders (Báez-Mendoza and Schultz, 2013; Prager and Plotkin, 2019; Zhai et al., 2018; Ztaou and Amalric, 2019). Concurrent metal increases could exacerbate neurotoxic consequences due to metal-metal interactions.

Levels of As, Se and Zn in exposed animals were well below currently known neurotoxic thresholds. However, it is possible that more prolonged exposures or higher exposure levels could result in exceedance of these thresholds.

Metal accumulation was also accompanied by essential metal depletion across the CNS. Remarkably, depending on the CNS area investigated, we observed the same metals (e.g. Se and Zn) being either increased (both bioaccumulated +50–100-fold in the anterior frontal cortex) or decreased (both −26–27% in the olfactory bulb). For each essential metal, maximal depletion was observed in the olfactory bulb for Se and Zn, anterior frontal cortex for Mn, ventral midbrain for Zn, and spinal cord for Cu (Table 2). Among those essential metal depletions, none reached levels previously described to be neurotoxic, though almost for Se and Cu.

In conclusion, the main neurotoxic risk of e-cigarette use identified in this experimental animal study pertains to metal accumulation in the striatum, the frontal cortex (anterior frontal cortex and motor-somatosensory cortex), and the ventral midbrain. These CNS areas known to be vulnerable to metal excess are involved in serious neurological disorders (e.g., bipolar disorders and depression) and neurodegenerative diseases (e.g., Alzheimer's, Parkinson's and Huntington's diseases) previously linked themselves to metal dyshomeostasis (Chen et al., 2016; Cicero et al., 2017; Sussulini and Hauser-Davis, 2018).

4.4. Limitations

A limitation of this study is the relatively small sample size. In this context, correcting for multiple comparisons, e.g. using the Bonferroni correction, is challenging. Moreover, the different brain tissues and metals are not independent from each other. Larger animal studies are needed to conduct more complex analyses.

4.5. Future studies

This manuscript demonstrates that sub-chronic exposure to e-cigarette aerosol can induce significant CNS metal dyshomeostasis. Additional studies are needed to investigate the neurotoxic consequences of the e-cigarette aerosol-mediated metal accumulations in the CNS at the behavioral and pathological levels. Future work should investigate whether chronic exposure to e-cigarette aerosol leads to neuroinflammation, neurodegeneration and influences the expression and or the activity of enzymes involved in metal metabolism. Other neurotoxic components in e-cigarette aerosol include aldehydes and nicotine, and the health impacts of these compounds together with metals needs to be untangled to identify the e-cigarette aerosol components and mixtures with highest neurotoxic risk. Findings from our study may enable public health authorities and policy makers to evaluate the potential detrimental human health effects of neurotoxic metal exposures from e-cigarette use, as well as inform e-cigarette users and bystanders about potential neurotoxic health risks.

Supplementary Material

Refer to Web version on PubMed Central for supplementary material.

Funding

Research reported in this publication was supported by the NIEHS and the FDA Center for Tobacco Products (CTP) grant R21ES029777 (MH, NJK), and by NIEHS grant P30ES009089 (ANA, DBR, MH, NJK). The content is solely the responsibility of the authors and does not necessarily represent the official views of the NIH or the FDA.

Abbreviations:

As	Arsenic
C	Carbon
Cr	Chromium
Cu	Copper

Ga	Gallium
Ir	Iridium
Pb	Lead
Lu	Lutetium
Hg	Mercury
Mn	Manganese
Ni	Nickel
QC	quality control
Rh	rhodium
Sb	Antimony
Se	Selenium
Si	Silicon
Sn	Tin
Sr	Strontium
Tl	Thallium
U	Uranium
V	Vanadium
W	Tungsten
Zn	Zinc
CNS	Central Nervous System
DRC	dynamic reaction cell
ICP-MS	inductively coupled plasma mass spectrometry
MDL	Method detection limits
MQL	Method quantitation limits

References

Alasmari F, Crotty Alexander LE, Nelson JA, Schiefer IT, Breen E, Drummond CA, Sari Y, 2017. Effects of chronic inhalation of electronic cigarettes containing nicotine on glial glutamate transporters and α-7 nicotinic acetylcholine receptor in female CD-1 mice. Prog. Neuro-Psychopharmacology Biol. Psychiatry 77, 1–8. 10.1016/j.pnpbp.2017.03.017

Alexander GE, DeLong MR, Strick PL, 1986. Parallel organization of functionally segregated circuits linking basal ganglia and cortex. Annu. Rev. Neurosci VOL. 9, 357–381. 10.1146/annurev.ne.09.030186.002041 [PubMed: 3085570]

Alpdogan S, Neumaier F, Hescheler J, Albanna W, Schneider T, 2020. Experimentally Induced Convulsive Seizures Are Modulated in Part by Zinc Ions through the Pharmacoresistant Cav2.3 Calcium Channel. Cell. Physiol. Biochem 54, 180–194. 10.33594/000000213 [PubMed: 32068980]

Antonini JM, Roberts JR, Chapman RS, Soukup JM, Ghio AJ, Sriram K, 2010. Pulmonary toxicity and extrapulmonary tissue distribution of metals after repeated exposure to different welding fumes. Inhal. Toxicol 22, 805–816. 10.3109/08958371003621641 [PubMed: 20560776]

ATSDR, 2012. TOXICOLOGICAL PROFILE FOR MANGANESE.

Badea M, Luzardo OP, González-Antuña A, Zumbado M, Rogozea L, Floroian L, Alexandrescu D, Moga M, Gaman L, Radoi M, Boada LD, Henríquez-Hernández LA, 2018. Body burden of toxic metals and rare earth elements in non-smokers, cigarette smokers and electronic cigarette users. Environ. Res 166, 269–275. 10.1016/j.envres.2018.06.007 [PubMed: 29908458]

Báez-Mendoza R, Schultz W, 2013. The role of the striatum in social behavior. Front. Neurosci 7, 233. 10.3389/fnins.2013.00233 [PubMed: 24339801]

Bartholomew RA, Li H, Gaidis EJ, Stackmann M, Shoemaker CT, Rossi MA, Yin HH, 2016. Striatonigral control of movement velocity in mice. Eur. J. Neurosci 43, 1097–1110. 10.1111/ejn.13187 [PubMed: 27091436]

Beyer H, 1981. Tukey, John W.: Exploratory Data Analysis. Addison-Wesley Publishing Company Reading, Mass. — Menlo Park, Cal., London, Amsterdam, Don Mills, Ontario, Sydney 1977, XVI, 688 S. Biometrical J. 23, 413–414. 10.1002/bimj.4710230408

Bizon JL, Foster TC, Alexander GE, Glisky EL, 2012. Characterizing cognitive aging of working memory and executive function in animal models. Front. Aging Neurosci 4, 19. 10.3389/fnagi.2012.00019 [PubMed: 22988438]

Bjørklund G, Dadar M, Chirumbolo S, Aaseth J, 2020. The Role of Xenobiotics and Trace Metals in Parkinson's Disease. Mol. Neurobiol 57, 1405–1417. 10.1007/s12035-019-01832-1 [PubMed: 31754997]

Block ML, Elder A, Auten RL, Bilbo SD, Chen H, Chen JC, Cory-Slechta DA, Costa D, Diaz-Sanchez D, Dorman DC, Gold DR, Gray K, Jeng HA, Kaufman JD, Kleinman MT, Kirshner A, Lawler C, Miller DS, Nadadur SS, Ritz B, Semmens EO, Tonelli LH, Veronesi B, Wright RO, Wright RJ, 2012. The outdoor air pollution and brain health workshop. Neurotoxicology 33, 972–984. 10.1016/j.neuro.2012.08.014 [PubMed: 22981845]

Bowman AB, Kwakye GF, Herrero Hernández E, Aschner M, 2011. Role of manganese in neurodegenerative diseases. J. Trace Elem. Med. Biol 25, 191–203. 10.1016/j.jtemb.2011.08.144 [PubMed: 21963226]

Brewer GJ, Yuzbasiyan-Gurkan V, 1992. Wilson disease. Med. (United States) 71, 139–164. 10.1097/00005792-199205000-00004

Brikmanis K, Petersen A, Doran N, 2017. E-cigarette use, perceptions, and cigarette smoking intentions in a community sample of young adult nondaily cigarette smokers. Psychol. Addict. Behav 31, 336–342. 10.1037/adb0000257 [PubMed: 28125242]

Bulcke F, Dringen R, Scheiber IF, 2017. Neurotoxicity of Copper. Adv. Neurobiol 18, 313–343. 10.1007/978-3-319-60189-2_16 [PubMed: 28889275]

Burdo JR, Martin J, Menzies SL, Dolan KG, Romano MA, Fletcher RJ, Garrick MD, Garrick LM, Connor JR, 1999. Cellular distribution of iron in the brain of the Belgrade rat. Neuroscience 93, 1189–1196. 10.1016/S0306-4522(99)00207-9 [PubMed: 10473284]

Caito S, Aschner M, 2017. Developmental Neurotoxicity of Lead. Adv. Neurobiol 18, 3–12. 10.1007/978-3-319-60189-2_1 [PubMed: 28889260]

Campos-Escamilla C, 2021. The role of transferrins and iron-related proteins in brain iron transport: applications to neurological diseases. Adv. Protein Chem. Struct. Biol 123, 133–162. 10.1016/bs.apcsb.2020.09.002 [PubMed: 33485481]

Cardenia V, Vivarelli F, Cirillo S, Paolini M, Canistro D, Rodriguez-Estrada MT, 2018. The effect of electronic-cigarettes aerosol on rat brain lipid profile. Biochimie 153, 99–108. 10.1016/j.biochi.2018.07.027 [PubMed: 30077815]

Cesbron A, Saussereau E, Mahieu LL, Couland I, Guerbet M, Goulle J-P, Goullé JP, 2013. Metallic profile of whole blood and plasma in a series of 106 healthy volunteers. J. Anal. Toxicol 37, 401–405. 10.1093/jat/bkt046 [PubMed: 23794607]

Chen H, Li G, Chan YL, Nguyen T, van Reyk D, Saad S, Oliver BG, 2018. Modulation of neural regulators of energy homeostasis, and of inflammation, in the pups of mice exposed to e-cigarettes. Neurosci. Lett 684, 61–66. 10.1016/j.neulet.2018.07.001 [PubMed: 29981356]

Chen KLB, Amarasiriwardena CJ, Christiani DC, 1999. Determination of total arsenic concentrations in nails by inductively coupled plasma mass spectrometry. Biol. Trace Elem. Res 67, 109–125. 10.1007/BF02784067 [PubMed: 10073418]

Chen P, Miah MR, Aschner M, 2016. Metals and Neurodegeneration. F1000Research 5, 366. 10.12688/f1000research.7431.1

Chowdhury TR, Samanta G, Chowdhury PP, Chanda C, Basu G, Lodh D, Nndi S, Chakraborty T, Mandal S, Bhattacharyua SM, Chakraborti D, 1997. Arsenic in groundwater in six districts of West Bengal, India: the biggest arsenic calamity in the world: the status report up to August, 1995, Arsenic. Springer, Dordrecht. 10.1039/AN994190168N

Cicero CE, Mostile G, Vasta R, Rapisarda V, Signorelli SS, Ferrante M, Zappia M, Nicoletti A, 2017. Metals and neurodegenerative diseases. A systematic review. Environ. Res 159, 82–94. 10.1016/j.envres.2017.07.048 [PubMed: 28777965]

Cilliers K, Muller CJF, 2020. Multi-element Analysis of Brain Regions from South African Cadavers. Biol. Trace Elem. Res 199, 425–441. 10.1007/s12011-020-02158-z [PubMed: 32361883]

Crotty Alexander LE, Drummond CA, Hepokoski M, Mathew D, Moshensky A, Willeford A, Das S, Singh P, Yong Z, Lee JH, Vega K, Du A, Shin J, Javier C, Tian J, Brown JH, Breen EC, 2018. Chronic inhalation of e-cigarette vapor containing nicotine disrupts airway barrier function and induces systemic inflammation and multiorgan fibrosis in mice. Am. J. Physiol. - Regul. Integr. Comp. Physiol 314, R834–R847. 10.1152/ajpregu.00270.2017 [PubMed: 29384700]

Czogala J, Goniewicz ML, Fidelus B, Zielinska-Danch W, Travers MJ, Sobczak A, 2014. Secondhand Exposure to Vapors From Electronic Cigarettes. Nicotine Tob. Res 16, 655–662. 10.1093/ntr/ntt203 [PubMed: 24336346]

Dankovic DA, Naumann BD, Maier A, Dourson ML, Levy LS, 2015. The Scientific Basis of Uncertainty Factors Used in Setting Occupational Exposure Limits. J. Occup. Environ. Hyg 12, S55–S68. 10.1080/15459624.2015.1060325 [PubMed: 26097979]

Deane R, Bradbury MWB, 1990. Transport of Lead- 203 at the Blood- Brain Barrier During Short Cerebrovascular Perfusion with Saline in the Rat. J. Neurochem 54, 905–914. 10.1111/j.1471-4159.1990.tb02337.x [PubMed: 2106011]

Dorne JLCM, Renwick AG, 2005. The refinement of uncertainty/safety factors in risk assessment by the incorporation of data on toxicokinetic variability in humans. Toxicol. Sci 86, 20–6. 10.1093/toxsci/kfi160 [PubMed: 15800035]

Ebbesen CL, Insanally MN, Kopec CD, Murakami M, Saiki A, Erlich JC, 2018. More than just a “motor”: Recent surprises from the frontal cortex. J. Neurosci 38, 9402–9413. 10.1523/JNEUROSCI.1671-18.2018 [PubMed: 30381432]

Elder A, Gelein R, Silva V, Feikert T, Opanashuk L, Carter J, Potter R, Maynard A, Ito Y, Finkelstein J, Oberdörster G, 2006. Translocation of inhaled ultrafine manganese oxide particles to the central nervous system. Environ. Health Perspect 114, 1172–1178. 10.1289/ehp.9030 [PubMed: 16882521]

Elsenhans B, Schmolke G, Kolb K, Stokes J, Forth W, 1987. Metal-metal interactions among dietary toxic and essential trace metals in the rat. Ecotoxicol. Environ. Saf 14, 275–287. 10.1016/0147-6513(87)90071-6 [PubMed: 3691380]

Farsalinos K, Romagna G, Allifranchini E, Ripamonti E, Bocchietto E, Todeschi S, Tsiapras D, Kyrzopoulos S, Voudris V, 2013. Comparison of the Cytotoxic Potential of Cigarette Smoke and Electronic Cigarette Vapour Extract on Cultured Myocardial Cells. Int. J. Environ. Res. Public Health 10, 5146–5162. 10.3390/ijerph10105146 [PubMed: 24135821]

Fernsebner K, Zorn J, Kanawati B, Walker A, Michalke B, 2014. Manganese leads to an increase in markers of oxidative stress as well as to a shift in the ratio of Fe(ii)/(iii) in rat brain tissue. Metallomics 6, 921–931. 10.1039/c4mt00022f [PubMed: 24599255]

Ferrea S, Winterer G, 2009. Neuroprotective and Neurotoxic Effects of Nicotine. Pharmacopsychiatry 42, 255–265. 10.1055/s-0029-1224138 [PubMed: 19924585]

Field A, 2013. Discovering Statistics Using IBM SPSS Statistics, 4th ed. SAGE, London.

Fitsanakis VA, Zhang N, Garcia S, Aschner M, 2010. Manganese (Mn) and iron (Fe): Interdependency of transport and regulation. Neurotox. Res 18, 124–131. 10.1007/s12640-009-9130-1 [PubMed: 19921534]

Frazzini V, Granzotto A, Bomba M, Massetti N, Castelli V, D'Aurora M, Punzi M, Iorio M, Mosca A, Delli Pizzi S, Gatta V, Cimini A, Sensi SL, 2018. The pharmacological perturbation of brain zinc impairs BDNF-related signaling and the cognitive performances of young mice. Sci. Rep 8. 10.1038/s41598-018-28083-9

Fredriksson A, Archer T, 2003. Effect of postnatal iron administration on MPTP-induced behavioral deficits and neurotoxicity: Behavioral enhancement by L-Dopa-MK-801 co-administration. Behav. Brain Res 139, 31–46. 10.1016/S0166-4328(02)00035-9 [PubMed: 12642174]

Gardner B, Dieriks BV, Cameron S, Mendis LHS, Turner C, Faull RLM, Curtis MA, 2017. et al. Metal concentrations and distributions in the human olfactory bulb in Parkinson's disease. Sci. Rep 7, 10454. 10.1038/s41598-017-10659-6 [PubMed: 28874699]

Ghaderi A, NasehGhafoori P, Rasouli-Azad M, Sehat M, Mehrzad F, Nekuei M, Aaseth J, Banafshe HR, Mehrpour O, 2018. Examining of Thallium in Cigarette Smokers. Biol. Trace Elem. Res 182, 224–230. 10.1007/s12011-017-1107-y [PubMed: 28766107]

Giedd JN, 2008. The Teen Brain: Insights from Neuroimaging. J. Adolesc. Heal 42, 335–343. 10.1016/j.jadohealth.2008.01.007

Glynos C, Bibli S-I, Katsaounou P, Pavlidou A, Magkou C, Karavana V, Topouzis S, Kalomenidis I, Zakynthinos S, Papapetropoulos A, 2018. Comparison of the effects of e-cigarette vapor with cigarette smoke on lung function and inflammation in mice. Am. J. Physiol. Cell. Mol. Physiol 315, L662–L672. 10.1152/ajplung.00389.2017

Halabi C, Halabi A, Dean DL, Wang PN, Boxer AL, Trojanowski JQ, Dearmond SJ, Miller BL, Kramer JH, Seeley WW, 2013. Patterns of striatal degeneration in frontotemporal dementia. Alzheimer Dis. Assoc. Disord 27, 74–83. 10.1097/WAD.0b013e31824a7df4 [PubMed: 22367382]

Han Yongsheng, Dong J, Xu C, Rao R, Shu S, Li G, Cheng N, Wu Y, Yang H, Han Yongzhu, Zhong K, 2020. Application of 9.4T MRI in Wilson Disease Model TX Mice With Quantitative Susceptibility Mapping to Assess Copper Distribution. Front. Behav. Neurosci 14, 59. 10.3389/fnbeh.2020.00059 [PubMed: 32390811]

He M. Di, Xu SC, Zhang Xin, Wang Y, Xiong JC, Zhang Xiao, Lu YH, Zhang L, Yu ZP, Zhou Z, 2013. Disturbance of aerobic metabolism accompanies neurobehavioral changes induced by nickel in mice. Neurotoxicology 38, 9–16. 10.1016/j.neuro.2013.05.011 [PubMed: 23727075]

Hegarty SV, Sullivan AM, O'Keeffe GW, 2013. Midbrain dopaminergic neurons: A review of the molecular circuitry that regulates their development. Dev. Biol 379, 123–138. 10.1016/j.ydbio.2013.04.014 [PubMed: 23603197]

Heldt NA, Seliga A, Winfield M, Gajghate S, Reichenbach N, Yu X, Rom S, Tenneti A, May D, Gregory BD, Persidsky Y, 2020. Electronic cigarette exposure disrupts blood-brain barrier integrity and promotes neuroinflammation. Brain. Behav. Immun 88, 363–380. 10.1016/j.bbi.2020.03.034 [PubMed: 32243899]

Hess CA, Olmedo P, Navas-Acien A, Goessler W, Cohen JE, Rule AM, 2017. E-cigarettes as a source of toxic and potentially carcinogenic metals. Environ. Res 152, 221–225. 10.1016/j.envres.2016.09.026 [PubMed: 27810679]

Hilpert M, Ilievski V, Coady M, Andrade-Gutierrez M, Yan B, Chillrud SN, Navas-Acien A, Kleiman NJ, 2019. A custom-built low-cost chamber for exposing rodents to e-cigarette aerosol: practical considerations. Inhal. Toxicol 31, 399–408. 10.1080/08958378.2019.1698678 [PubMed: 31797690]

Hilpert M, Ilievski V, Hsu SY, Rule AM, Olmedo P, Drazer G, 2021. E-cigarette aerosol collection using converging and straight tubing Sections: Physical mechanisms. J. Colloid Interface Sci 584, 804–815. 10.1016/j.jcis.2020.10.011 [PubMed: 33268068]

Hintiryan H, Atlas OD, Gou HHL, Zingg B, Yamashita S, Lyden HM, Song MY, Grewal AK, Zhang X, Toga AW, Dong HW, 2012. Comprehensive connectivity of the mouse main olfactory bulb: Analysis and online digital atlas. Front. Neuroanat 6, 30. 10.3389/fnana.2012.00030 [PubMed: 22891053]

Imam SZ, Lantz-McPeak SM, Cuevas E, Rosas-Hernandez H, Liachenko S, Zhang Y, Sarkar S, Ramu J, Robinson BL, Jones Y, Gough B, Paule MG, Ali SF, Binienda ZK, 2015. Iron Oxide Nanoparticles Induce Dopaminergic Damage: In vitro Pathways and In Vivo Imaging Reveals Mechanism of Neuronal Damage. Mol. Neurobiol 52, 913–926. 10.1007/s12035-015-9259-2 [PubMed: 26099304]

Ingrassia R, Garavaglia B, Memo M, 2019. DMT1 Expression and iron levels at the crossroads between aging and neurodegeneration. Front. Neurosci 13, 575. 10.3389/fnins.2019.00575 [PubMed: 31231185]

Jackson-Lewis V, Przedborski S, 2007. Protocol for the MPTP mouse model of Parkinson's disease. Nat. Protoc 2, 141–151. 10.1038/nprot.2006.342 [PubMed: 17401348]

Jamal A, Gentzke A, Hu SS, Cullen KA, Apelberg BJ, Homa DM, King BA, 2017. Tobacco Use Among Middle and High School Students - United States, 2011–2016. MMWR. Morb. Mortal. Wkly. Rep 66, 597–603. 10.15585/mmwr.mm6623a1 [PubMed: 28617771]

Jiang H, Song N, Jiao Q, Shi L, Du X, 2019. Iron pathophysiology in parkinson diseases, in: Advances in Experimental Medicine and Biology. Springer New York LLC, pp. 45–66. 10.1007/978-981-13-9589-5_4

Johnson AR, Armstrong WD, Singer L, 1968. The incorporation and removal of large amounts of strontium by physiologic mechanisms in mineralized tissues of the rat. Calcif. Tissue Res 2, 242–252. 10.1007/BF02279212 [PubMed: 5748355]

Kaisar MA, Prasad S, Liles T, Cucullo L, 2016. A decade of e-cigarettes: Limited research & unresolved safety concerns. Toxicology 365, 67–75. 10.1016/j.tox.2016.07.020 [PubMed: 27477296]

Kaisar MA, Villalba H, Prasad S, Liles T, Sifat AE, Sajja RK, Abbruscato TJ, Cucullo L, 2017. Offsetting the impact of smoking and e-cigarette vaping on the cerebrovascular system and stroke injury: Is Metformin a viable countermeasure? Redox Biol. 13, 353–362. 10.1016/j.redox.2017.06.006 [PubMed: 28646795]

Kanti Das T, Wati MR, Fatima-Shad K, 2014. Oxidative Stress Gated by Fenton and Haber Weiss Reactions and Its Association With Alzheimer's Disease. Arch. Neurosci 2, e60038. 10.5812/archneurosci.20078

Kozlowski H, Kolkowska P, Watly J, Krzywoszynska K, Potocki S, 2014. General Aspects of Metal Toxicity. Curr. Med. Chem 21, 3721–3740. 10.2174/0929867321666140716093838 [PubMed: 25039781]

Krishna S, Dodd CA, Hekmatyar SK, Filipov NM, 2014. Brain deposition and neurotoxicity of manganese in adult mice exposed via the drinking water. Arch. Toxicol 88, 47–64. 10.1007/s00204-013-1088-3 [PubMed: 23832297]

Kuntic M, Oelze M, Steven S, Kröller-Schön S, Stamm P, Kalinovic S, Frenis K, Vujacic-Mirski K, Bayo Jimenez MT, Kvandova M, Filippou K, Al Zuabi A, Brückl V, Hahad O, Daub S, Varveri F, Gori T, Huesmann R, Hoffmann T, Schmidt FP, Keaney JF, Daiber A, Münzel T, 2020. Short-term e-cigarette vapour exposure causes vascular oxidative stress and dysfunction: evidence for a close connection to brain damage and a key role of the phagocytic NADPH oxidase (NOX-2). Eur. Heart J 41, 2472–2483. 10.1093/eurheartj/ehz772 [PubMed: 31715629]

Larcombe AN, Janka MA, Mullins BJ, Berry LJ, Bredin A, Franklin PJ, 2017. The effects of electronic cigarette aerosol exposure on inflammation and lung function in mice. Am. J. Physiol. Cell. Mol. Physiol 313, L67–L79. 10.1152/ajplung.00203.2016

Lauterstein D, Tijerina P, Corbett K, Akgol Oksuz B, Shen S, Gordon T, Klein C, Zelikoff J, 2016. Frontal Cortex Transcriptome Analysis of Mice Exposed to Electronic Cigarettes During Early Life Stages. Int. J. Environ. Res. Public Health 13, 417. 10.3390/ijerph13040417 [PubMed: 27077873]

Lee H-W, Park S-H, Weng M, Wang H-T, Huang WC, Lepor H, Wu X-R, Chen L-C, Tang M, 2018. E-cigarette smoke damages DNA and reduces repair activity in mouse lung, heart, and bladder as well as in human lung and bladder cells. Proc. Natl. Acad. Sci 115, E1560–E1569. 10.1073/pnas.1718185115 [PubMed: 29378943]

Lewis J, Bench G, Myers O, Tinner B, Staines W, Barr E, Divine KK, Barrington W, Karlsson J, 2005. Trigeminal uptake and clearance of inhaled manganese chloride in rats and mice. Neurotoxicology 26, 113–123. 10.1016/j.neuro.2004.06.005 [PubMed: 15527879]

Li N, Liu X, Zhang P, Qiao M, Li H, Li X, Zhang H, Yu Z, 2015. The effects of early life lead exposure on the expression of interleukin (IL) 1β, IL-6, and glial fibrillary acidic protein in the hippocampus of mouse pups. Hum. Exp. Toxicol 34, 357–363. 10.1177/0960327114529451 [PubMed: 25028260]

Lieberman H, 1941. Chrome Ulcerations of the Nose and Throat. N. Engl. J. Med 225, 132–133. 10.1056/nejm194107242250402

Lu Z, Marks E, Chen J, Moline J, Barrows L, Raisbeck M, Volitakis I, Cherny RA, Chopra V, Bush AI, Hersch S, Fox JH, 2014. Altered selenium status in Huntington's disease: Neuroprotection by selenite in the N171-82Q mouse model. Neurobiol. Dis 71, 34–42. 10.1016/j.nbd.2014.06.022 [PubMed: 25014023]

Lucchini RG, Dorman DC, Elder A, Veronesi B, 2012. Neurological impacts from inhalation of pollutants and the nose-brain connection. Neurotoxicology 33, 838–841. 10.1016/j.neuro.2011.12.001 [PubMed: 22178536]

Luo J. hua, Qiu Z. qun, Shu W. qun, Zhang Y. yan, Zhang L, Chen J. an, 2009. Effects of arsenic exposure from drinking water on spatial memory, ultra-structures and NMDAR gene expression of hippocampus in rats. Toxicol. Lett 184, 121–125. 10.1016/j.toxlet.2008.10.029 [PubMed: 19041379]

Meenakshi-Sundaram S, Mahadevan A, Taly AB, Arunodaya GR, Swamy HS, Shankar SK, 2008. Wilson's disease: A clinico-neuropathological autopsy study. J. Clin. Neurosci 15, 409–417. 10.1016/j.jocn.2006.07.017 [PubMed: 18242093]

Mehri A, 2020. Trace elements in human nutrition (II) - An update. Int. J. Prev. Med 11, 2. 10.4103/ijpvm.IJPVM_48_19 [PubMed: 32042399]

Minigalieva IA, Katsnelson BA, Privalova LI, Sutunkova MP, Gurvich VB, Shur VY, Shishkina EV, Valamina IE, Makeyev OH, Panov VG, Varaksin AN, Grigoryeva EV, Meshtcheryakova EY, 2015. Attenuation of combined nickel(II) oxide and manganese(II, III) oxide nanoparticles' adverse effects with a complex of bioprotectors. Int. J. Mol. Sci 16, 22555–22583. 10.3390/ijms160922555 [PubMed: 26393577]

Nguyen T, Li GE, Chen H, Cranfield CG, McGrath KC, Gorrie CA, 2018. Maternal E-Cigarette Exposure Results in Cognitive and Epigenetic Alterations in Offspring in a Mouse Model. Chem. Res. Toxicol 31, 601–611. 10.1021/acs.chemrestox.8b00084 [PubMed: 29863869]

Ngwa HA, Ay M, Jin H, Anantharam V, Kanthasamy A, Kanthasamy AG, 2017. Neurotoxicity of Vanadium. Adv. Neurobiol 18, 287–301. 10.1007/978-3-319-60189-2_14 [PubMed: 28889273]

Nixon D, Moyer T, 1996. Routine clinical determination of lead, arsenic, cadmium, and thallium in urine and whole blood by inductively coupled plasma mass spectrometry. Spectrochim. Acta Part B At. Spectrosc 51, 13–25.

Noël A, Verret CM, Hasan F, Lomnicki S, Morse J, Robichaud A, Penn AL, 2018. Generation of electronic cigarette aerosol by a third-generation machine-vaping device: application to toxicological studies. J. Vis. Exp 2018, 58095. 10.3791/58095

Nopoulos PC, 2016. Huntington disease: A single-gene degenerative disorder of the striatum. Dialogues Clin. Neurosci 18, 91–98. 10.31887/dcns.2016.18.1/pnopoulos [PubMed: 27069383]

Nudler SI, Quinteros FA, Miler EA, Cabilla JP, Ronchetti SA, Duvilanski BH, 2009. Chromium VI administration induces oxidative stress in hypothalamus and anterior pituitary gland from male rats. Toxicol. Lett 185, 187–192. 10.1016/j.toxlet.2009.01.003 [PubMed: 19167472]

Olmedo P, Goessler W, Tanda S, Grau-Perez M, Jarmul S, Aherrera A, Chen R, Hilpert M, Cohen JE, Navas-Acien A, Rule AM, 2018. Metal Concentrations in e-Cigarette Liquid and Aerosol Samples: The Contribution of Metallic Coils. Environ. Health Perspect 126, 027010. 10.1289/EHP2175 [PubMed: 29467105]

Olmedo P, Navas-Acien A, Hess C, Jarmul S, Rule A, 2016. A direct method for e-cigarette aerosol sample collection. Environ. Res 149, 151–156. 10.1016/j.envres.2016.05.008 [PubMed: 27200479]

Outridge PM, Scheuhammer AM, 1993. Bioaccumulation and toxicology of chromium: Implications for wildlife. Rev. Environ. Contam. Toxicol 130, 31–77. 10.1007/978-1-4613-9763-2_2 [PubMed: 8419988]

Panter KE, Hartley WJ, James LF, Mayland HF, Stegelmeier BL, Kechele PO, 1996. Comparative toxicity of selenium from Seleno-DL-methionine, sodium selenate, and Astragalus bisulcatus in pigs. Fundam. Appl. Toxicol 32, 217–223. 10.1006/faat.1996.0124 [PubMed: 8921324]

Pesko MF, Robarts AMT, 2017. Adolescent Tobacco Use in Urban Versus Rural Areas of the United States: The Influence of Tobacco Control Policy Environments. J. Adolesc. Heal 61, 70–76. 10.1016/j.jadohealth.2017.01.019

Petrilli FL, Rossi GA, Camoirano A, Romano M, Serra D, Bennicelli C, De Flora A, De Flora S, 1986. Metabolic reduction of chromium by alveolar macrophages and its relationships to cigarette smoke. J. Clin. Invest 77, 1917–1924. 10.1172/JCI112520 [PubMed: 2423559]

Portbury SD, Adlard PA, 2017. Zinc signal in brain diseases. Int. J. Mol. Sci 18, 2506. 10.3390/ijms18122506

Prager EM, Plotkin JL, 2019. Compartmental function and modulation of the striatum. J. Neurosci. Res 97, 1503–1514. 10.1002/jnr.24522 [PubMed: 31489687]

Pruszkowski E, Neubauer K, Thomas R, 1998. An overview of clinical applications by inductively coupled plasma mass spectrometry. At. Spectrosc 19, 111–115.

Qasim H, Karim ZA, Silva- Espinoza JC, Khasawneh FT, Rivera JO, Ellis CC, Bauer SL, Almeida IC, Alshbool FZ, 2018. Short- Term E- Cigarette Exposure Increases the Risk of Thrombogenesis and Enhances Platelet Function in Mice. J. Am. Heart Assoc 7, e009264. 10.1161/JAHA.118.009264 [PubMed: 30021806]

Richner M, Jager SB, Siupka P, Vaegter CB, 2017. Hydraulic extrusion of the spinal cord and isolation of dorsal root ganglia in rodents. J. Vis. Exp 119, 55226. 10.3791/55226

Rosen BP, Liu Z, 2009. Transport pathways for arsenic and selenium: A minireview. Environ. Int 35, 512–515. 10.1016/j.envint.2008.07.023 [PubMed: 18789529]

Rowell TR, Reeber SL, Lee SL, Harris RA, Nethery RC, Herring AH, Glish GL, Tarran R, 2017. Flavored e-cigarette liquids reduce proliferation and viability in the CALU3 airway epithelial cell line. Am. J. Physiol. Cell. Mol. Physiol 313, L52–L66. 10.1152/ajplung.00392.2016

Ruszkiewicz JA, Zhang Z, Gonçalves FM, Tizabi Y, Zelikoff JT, Aschner M, 2020. Neurotoxicity of e-cigarettes. Food Chem. Toxicol 138, 111245. 10.1016/j.fct.2020.111245 [PubMed: 32145355]

Saffari A, Daher N, Ruprecht A, De Marco C, Pozzi P, Boffi R, Hamad SH, Shafer MM, Schauer JJ, Westerdahl D, Sioutas C, 2014. Particulate metals and organic compounds from electronic and tobacco-containing cigarettes: comparison of emission rates and secondhand exposure. Environ. Sci. Process. Impacts 16, 2259–2267. 10.1039/C4EM00415A [PubMed: 25180481]

Salama A, Hegazy R, Hassan A, 2016. Intranasal chromium induces acute brain and lung injuries in rats: Assessment of different potential hazardous effects of environmental and occupational exposure to chromium and introduction of a novel pharmacological and toxicological animal model. PLoS One 11, e0168688. 10.1371/journal.pone.0168688 [PubMed: 27997619]

Schröder N, Fredriksson A, Vianna MRM, Roesler R, Izquierdo I, Archer T, 2001. Memory deficits in adult rats following postnatal iron administration. Behav. Brain Res 124, 77–85. 10.1016/S0166-4328(01)00236-4 [PubMed: 11423168]

Sifat AE, Vaidya B, Kaisar MA, Cucullo L, Abbruscato TJ, 2018. Nicotine & electronic cigarette (E-Cig) exposure decreases brain glucose utilization in ischemic stroke. J. Neurochem 147, 204–221. 10.1111/jnc.14561 [PubMed: 30062776]

Skoryna S, 1981. Effects of oral supplementation with stable strontium - PubMed. Can Med Assoc J. 125, 703–712. [PubMed: 6120036]

Song X, Fiati Kenston SS, Kong L, Zhao J, 2017. Molecular mechanisms of nickel induced neurotoxicity and chemoprevention. Toxicology 392, 47–54. 10.1016/j.tox.2017.10.006 [PubMed: 29032222]

Soule EK, Maloney SF, Spindle TR, Rudy AK, Hiler MM, Cobb CO, 2017. Electronic cigarette use and indoor air quality in a natural setting. Tob. Control 26, 109–112. 10.1136/tobaccocontrol-2015-052772 [PubMed: 26880745]

Stroh A, 1993. Determination of Pb and Cd in whole blood using isotope dilution ICP-MS. At. Spectrosc 379, 872–80. 10.1007/s00216-004-2654-6

Sunderman FW, 2001. Nasal toxicity, carcinogenicity, and olfactory uptake of metals. Ann. Clin. Lab. Sci 31, 3–24. https://doi.org/https://pubmed.ncbi.nlm.nih.gov/11314863/ [PubMed: 11314863]

Sussulini A, Hauser-Davis RA, 2018. Metallomics Applied to the Study of Neurodegenerative and Mental Diseases, Advances in Experimental Medicine and Biology. Springer New York LLC. 10.1007/978-3-319-90143-5_2

Takahashi S, Takahashi I, Sato H, Kubota Y, Yoshida S, Muramatsu Y, 2001. Age-Related Changes in the Concentrations of Major and Trace Elements in the Brain of Rats and Mice. Biol. Trace Elem. Res 80, 145–158. [PubMed: 11437180]

Tankersley CG, Fitzgerald RS, Kleeberger SR, 1994. Differential control of ventilation among inbred strains of mice. Am. J. Physiol. - Regul. Integr. Comp. Physiol 267, R1371–7. 10.1152/ajpregu.1994.267.5.r1371

Tonge K, 2017. The distribution of copper, zinc and iron in the brain and the implications for Alzheimer's disease. Fac. Sci. Med. Heal. - Honours Theses. University of Wollongong. https://doi.org/https://ro.uow.edu.au/thsci/140

Travacio M, Polo JM, Llesuy S, 2001. Chromium (VI) induces oxidative stress in the mouse brain. Toxicology 162, 139–148. 10.1016/S0300-483X(00)00423-6 [PubMed: 11337112]

Vinceti M, Mandrioli J, Borella P, Michalke B, Tsatsakis A, Finkelstein Y, 2014. Selenium neurotoxicity in humans: Bridging laboratory and epidemiologic studies. Toxicol. Lett 230, 295–303. 10.1016/j.toxlet.2013.11.016 [PubMed: 24269718]

Watanabe C, Satoh H, 1994. Brain selenium status and behavioral development in selenium-deficient preweanling mice. Physiol. Behav 56, 927–932. 10.1016/0031-9384(94)90325-5 [PubMed: 7824593]

Wharton JD, Kozek LK, Carson RP, 2020. Increased Seizure Frequency Temporally Related to Vaping: Where There's Vapor, There's Seizures? Pediatr. Neurol 104, 66–67. 10.1016/j.pediatrneurol.2019.10.006 [PubMed: 31917097]

Whitcomb BW, Schisterman EF, 2008. Assays with lower detection limits: Implications for epidemiological investigations. Paediatr. Perinat. Epidemiol 22, 597–602. 10.1111/j.1365-3016.2008.00969.x [PubMed: 19000298]

Williams M, Bozhilov K, Ghai S, Talbot P, 2017. Elements including metals in the atomizer and aerosol of disposable electronic cigarettes and electronic hookahs. PLoS One 12, e0175430. 10.1371/journal.pone.0175430 [PubMed: 28414730]

Williams M, Villarreal A, Bozhilov K, Lin S, Talbot P, 2013. Metal and Silicate Particles Including Nanoparticles Are Present in Electronic Cigarette Cartomizer Fluid and Aerosol. PLoS One 8, e57987. 10.1371/journal.pone.0057987 [PubMed: 23526962]

Wu J, Ding T, Sun J, 2013. Neurotoxic potential of iron oxide nanoparticles in the rat brain striatum and hippocampus. Neurotoxicology 34, 243–253. 10.1016/j.neuro.2012.09.006 [PubMed: 22995439]

Yang Y, Jing XP, Zhang SP, Gu RX, Tang FX, Wang XL, Xiong Y, Qiu M, Sun XY, Ke D, Wang JZ, Liu R, 2013. High Dose Zinc Supplementation Induces Hippocampal Zinc Deficiency and Memory Impairment with Inhibition of BDNF Signaling. PLoS One 8. 10.1371/journal.pone.0055384

Ye Q, Kim J, 2016. Mutation in HFE gene decreases manganese accumulation and oxidative stress in the brain after olfactory manganese exposure. Metallomics 8, 618. 10.1039/C6MT00080K [PubMed: 27295312]

Yokel RA, Crossgrove JS, Bukaveckas BL, 2003. Manganese distribution across the blood-brain barrier. II. Manganese efflux from the brain does not appear to be carrier mediated. Neurotoxicology 24, 15–22. 10.1016/S0161-813X(02)00090-6 [PubMed: 12564378]

Zelikoff JT, Parmalee NL, Corbett K, Gordon T, Klein CB, Aschner M, 2018. Microglia Activation and Gene Expression Alteration of Neurotrophins in the Hippocampus Following Early-Life Exposure to E-Cigarette Aerosols in a Murine Model. Toxicol. Sci 162, 276–286. 10.1093/toxsci/kfx257 [PubMed: 29161446]

Zhai S, Tanimura A, Graves SM, Shen W, Surmeier DJ, 2018. Striatal synapses, circuits, and Parkinson's disease. Curr. Opin. Neurobiol 48, 9–16. 10.1016/j.conb.2017.08.004 [PubMed: 28843800]

Zhang S, Wang Xuefeng, Wang Xiaohui, Shen X, Sun J, Hu X, Chen P, 2017. Sr2+ has low efficiency in regulating spontaneous release at the Calyx of Held synapses. Synapse 71, 11. 10.1002/syn.21983

Zhang Y, Zhou Y, Schweizer U, Savaskan NE, Hua D, 2008. Comparative Analysis of Selenocysteine Machinery and Selenoproteome Gene Expression in Mouse Brain Identifies Neurons as Key Functional Sites of Selenium in Mammals 283, 2427–38. 10.1074/jbc.M707951200

Zhao D, Aravindakshan A, Hilpert M, Olmedo P, Rule AM, Navas-Acien A, Aherrera A, 2020. Metal/metalloid levels in electronic cigarette liquids, aerosols, and human biosamples: A systematic review. Environ. Health Perspect 128, 36001. 10.1289/EHP5686 [PubMed: 32186411]

Zhao D, Navas-Acien A, Ilievski V, Slavkovich V, Olmedo P, Adria-Mora B, Domingo-Relloso A, Aherrera A, Kleiman NJ, Rule AM, Hilpert M, 2019. Metal concentrations in electronic cigarette aerosol: Effect of open-system and closed-system devices and power settings. Environ. Res 174, 125–134. 10.1016/j.envres.2019.04.003 [PubMed: 31071493]

Zheng W, Aschner M, Ghersi-Egea JF, 2003. Brain barrier systems: A new frontier in metal neurotoxicological research. Toxicol. Appl. Pharmacol 192, 1–11. 10.1016/S0041-008X(03)00251-5 [PubMed: 14554098]

Zhou G, Lane G, Cooper SL, Kahnt T, Zelano C, 2019. Characterizing functional pathways of the human olfactory system. Elife 8. 10.7554/eLife.47177

Ztaou S, Amalric M, 2019. Contribution of cholinergic interneurons to striatal pathophysiology in Parkinson's disease. Neurochem. Int 126, 1–10. 10.1016/j.neuint.2019.02.019 [PubMed: 30825602]

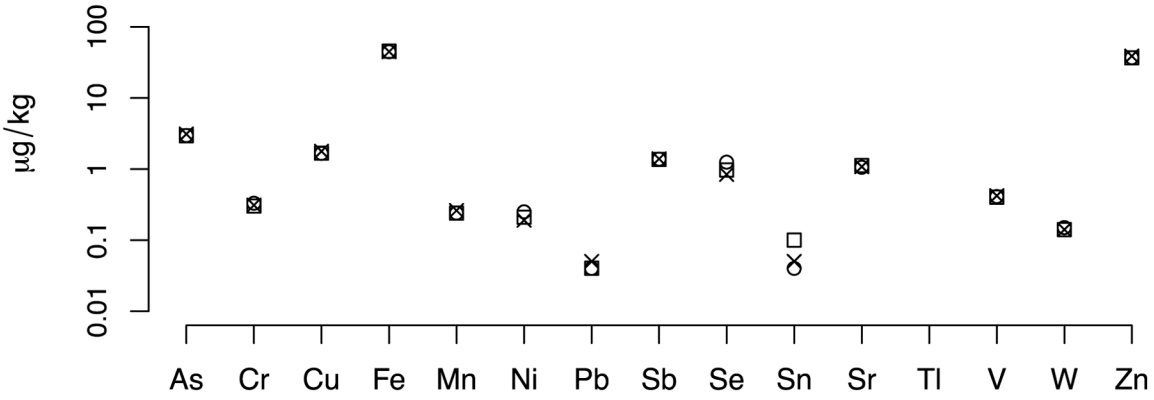

Figure 1: E-cigarette aerosol metal content.

The levels of 15 metals/metalloids in e-cigarette aerosol were measured by ICP-MS using the identical e-cigarette device, coil type and puff/interpuff timing as that used in the animal exposures. The three different symbols (□o x) depict results from three independent measurements.

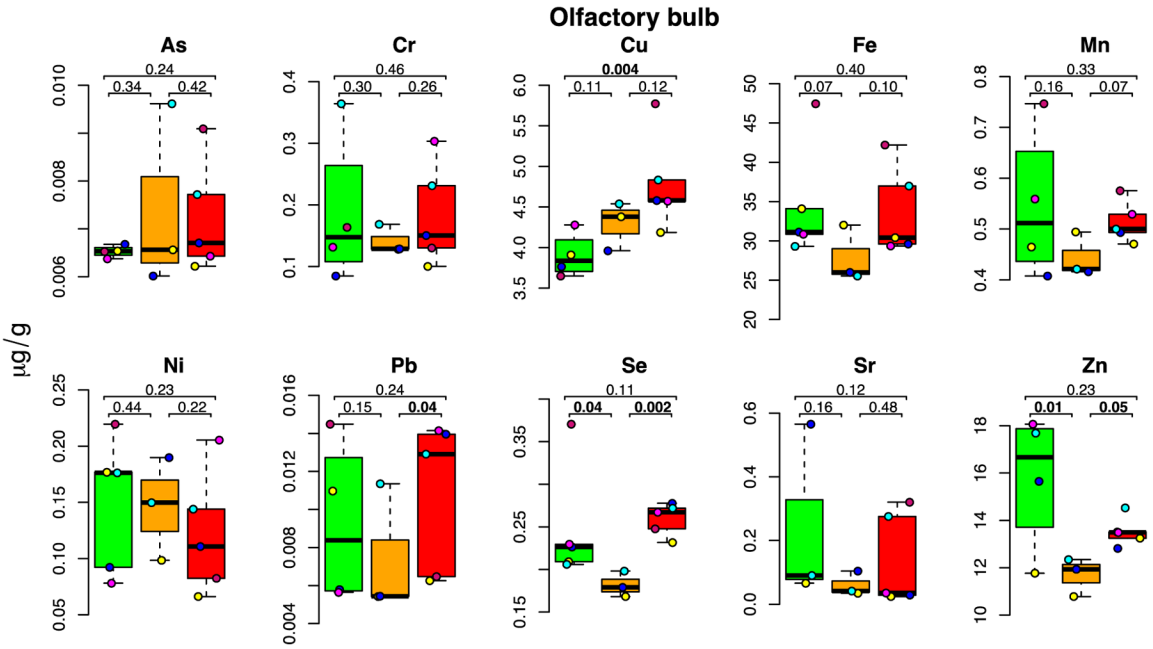

Figure 2: E-cigarette aerosol-mediated metal level changes in the olfactory bulb.

For each metal, box plots are shown for metal concentrations measured in the five mice in the control (green), low dose (orange) and high dose (red) exposure groups. Each individual mouse within a group is identified by a different color. For each box plot, the number of samples (after outlier removal) ranges between 3 and 5 as indicated by the number of datapoints. Height of box delineates inter quartile range, and the horizontal line the median. Below MDL measurements are indicated by a square, above MDL by a circle.

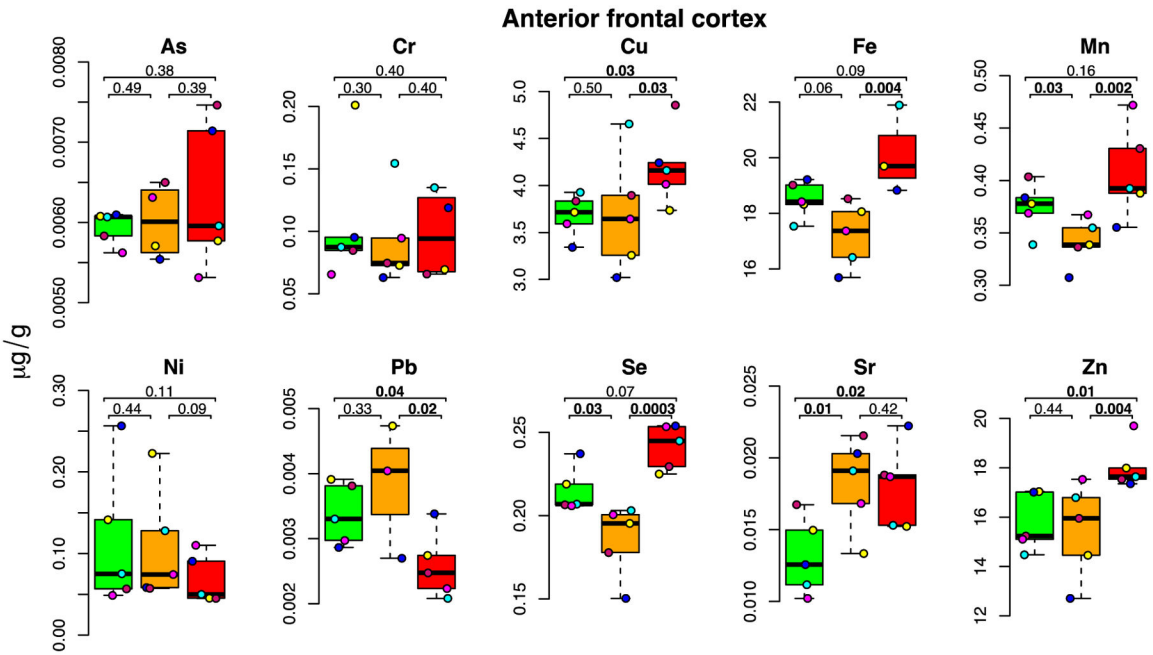

Figure 3: E-cigarette aerosol-mediated metal level changes in the anterior frontal cortex.

For each metal, box plots are shown for metal concentrations measured in the five mice in the control (green), low dose (orange) and high dose (red) exposure groups. Each individual mouse within a group is identified by a different color. The number of samples (after outlier removal) ranges between 3 and 5 for each box plot as indicated by the number of datapoints. Below MDL measurements are indicated by a square, above MDL by a circle.

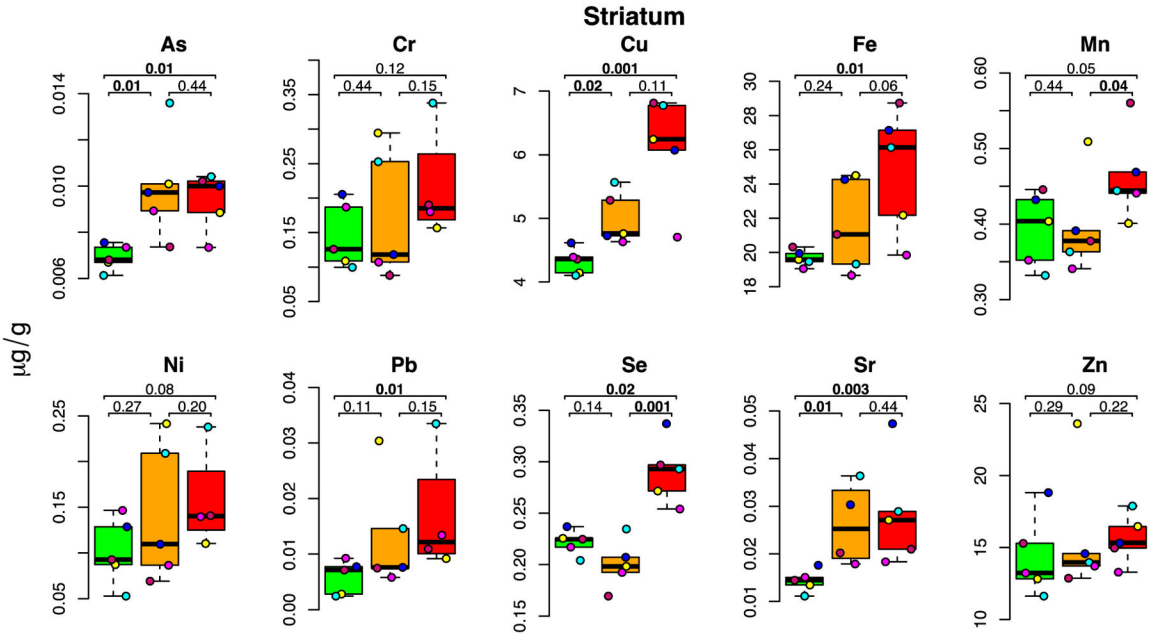

Figure 4: E-cigarette aerosol-mediated metal level changes in the striatum.

For each metal, box plots are shown for metal concentrations measured in the five mice in the control (green), low dose (orange) and high dose (red) exposure groups. Each individual mouse within a group is identified by a different color. The number of samples (after outlier removal) ranges between 4 and 5 for each box plot as indicated by the number of datapoints. Below MDL measurements are indicated by a square, above MDL by a circle.

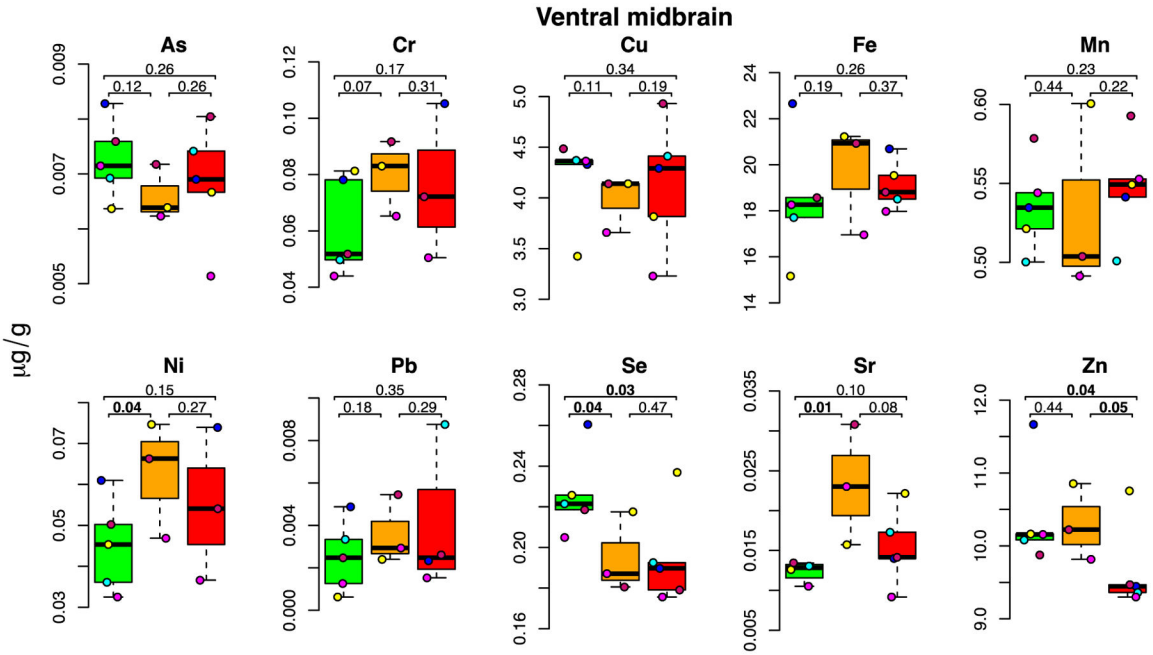

Figure 5: E-cigarette aerosol-mediated metal level changes in the ventral midbrain.

For each metal, box plots are shown for metal concentrations measured in the five mice in the control (green), low dose (orange) and high dose (red) exposure groups. Each individual a mouse within group is identified by a different color. The number of samples (after outlier removal) ranges between 3 and 5 for each box plot as indicated by the number of datapoints. Below MDL measurements are indicated by a square, above MDL by a circle.

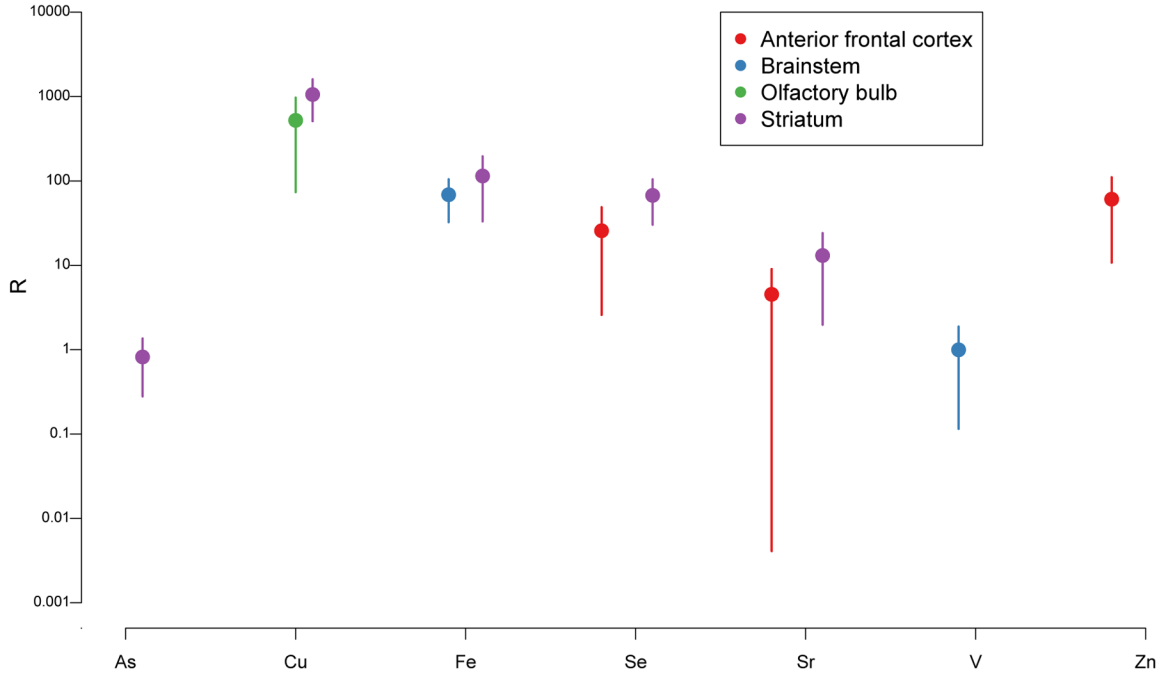

Figure 6: Partitioning ratio *R*.

This ratio defined in Equation (1) quantifies the ratio between the mean metal level in a given tissue type from mice exposed to the high e-cigarette dose (relative to mean metal level in the control group) and the aerosol metal level. High *R* values indicate bio-accumulation. Vertical bars indicate 95% confidence intervals. Values are shown only for metal-tissue combinations for which *R* is significantly positive.

Table 1:

Mouse blood metal levels at the end of the 2-month exposure.

Mean (standard deviation) of the concentrations of 10 metals measured by ICP-MS in mouse blood are reported here.

	Control	Low dose	High dose
As	3.10 (0.23)	2.77 (0.38)	3.22 (0.48)
Cr	1.37 (0.02)	**1.93 (0.50)***	**1.79 (0.36)***
Cu	565 (43)	587 (11)	565 (20)
Fe	323371 (20557)	330330 (21408)	**345403 (7497)***
Mn	8.53 (1.61)	**10.89 (0.19)***	9.48 (0.11)
Ni	3.25 (0.65)	3.69 (0.06)	4.22 (1.49)
Pb	1.29 (0.73)	1.65 (0.66)	**0.85 (0.05)***
Se	535 (33)	**591 (55)***	562 (67)
Sr	16.5 (1.9)	17.4 (2.0)	17.9 (0.2)
Zn	4666 (565)	4381 (308)	5101 (666)

Data are expressed in μg/L. Boldface indicates a statistically significant difference between an exposed group and the control group.

Table 2:
Summary of measured metal changes and literature-predicted neurotoxic significance.

Ranges of metal levels detected in this study for each metal across groups (control and exposed) throughout the central nervous system (CNS) are given in μg/g of wet tissue (first column).

		Accumulation-induced toxicity			Depletion-induced toxicity		
	Range of levels μg/g) detected in our study	Max increase measured	Known published neurotoxic increase	Reference	Max decrease measured	Known published neurotoxic decrease	Reference
As	0.005–0.014	44% ST	1000%	Luo 2009	N/A	_	_
Cr	0.01–0.35	61% MSCx	60%	Travacio 2001; Salama 2016	N/A	_	_
Cu	2.5–7.0	42% ST	29%	Han 2020	−14% SC	−20%	Bulcke 2017
Fe	12–47	26% ST	16%	Schröder 2001; Fredricksson 2003	N/A	–	–
Mn	0.30–0.75	18% ST	19%	Krishna 2014	−9% AFCx	−33%	Moldovan 2015
Ni	0.01–0.25	39% VM	0–102%	Minigalieva 2015; He 2013	N/A	_	_
Pb	0.0005–0.0170	259% MSCx	200%	Li 2015	N/A		
Se	0.15–0.35	31% ST	150%	Panter 1996	−27% OB	−30%	Lu 2014; Watanabe 1994
Sr	0.007–0.600	99% ST	ND	Johnson 1968	N/A	_	_
Zn	8–24	14.5% AFCx	34%	Yang 2013	−26% OB	−50%	Frazzini 2018

The maximal significant increases and decreases we measured are expressed in % of unexposed controls with indication of the CNS areas where they were observed (AFCx=anterior frontal cortex; MSCx=motor-somatosensory cortex; OB=olfactory bulb; SC=spinal cord; ST=striatum; RB=remaining brain; VM=ventral midbrain). Known CNS (in most studies total brain) increases and decreases previously reported to be associated with neurotoxic outcomes for each metal are also indicated in % of unexposed controls. Shades of red indicate the level of predicted neurotoxic significance: dark red=changes predicted to have a high likelihood of neurotoxic impact based on published data demonstrating toxicity at levels equal or inferior to those measured in our study; salmon=changes predicted to have potential neurotoxic consequences based on published data indicating toxicity at levels close to those measured in our study, or based on the remarkable increase of a xenobiotic metal know to be neurotoxic without determination in the literature of neurotoxic brain levels (ND=not determined). Blank rows= changes are either not significant or far below published toxic levels or “not applicable N/A”, i.e., decrease in these metals is not predicted to have any adverse consequences based on the xenobiotic nature of the metal.